EFFECT OF METHYLMERCURY EXPOSURE ON HEART AND SKELETAL MUSCLE DEVELOPMENT IN ZEBRAFISH EMBRYOS (*DANIO RERIO*)

A Thesis

by

SONNY AGUILAR

Submitted to the Office of Graduate and Professional Studies of
Texas A&M University
in partial fulfillment of the requirements for the degree of

MASTER OF SCIENCE

Chair of Committee,	Louise C. Abbott
Committee Members,	Michelle D. Pine
	Mark J. Zoran
Head of Department,	Evelyn Tiffany-Castiglioni

December 2014

Major Subject: Biomedical Sciences

ABSTRACT

Mercury (Hg) in its elemental form is not effectively absorbed into the body until a methyl group is bound to an atom of Hg, creating methylmercury. Methylmercury (MeHg) is then readily absorbed from the digestive tract, and has demonstrated neurotoxic effects in both the developing and mature central nervous system (CNS). Previous studies have shown that exposure to high concentrations of MeHg results in both high morbidity and mortality rates demonstrated by cases of exposure in the Faroe Islands, Japan and Iraq. Common symptoms exhibited after high exposure to MeHg included sensory disturbances in adults, while children demonstrate anatomical abnormalities and cognitive defects. Recent zebrafish studies have demonstrated decreased hatching rate, movement, and length along with abnormal/disorganized skeletal muscle, and heart related problems. To better understand the neurotoxic mechanisms of MeHg on zebrafish development, we investigated overall embryo growth, various aspects of heart development, and neuromuscular junction (NMJ) development.

Using zebrafish embryos (ZFEs) as an animal model this study revealed that MeHg exposure for 24 hours had an effect on ZFEs, resulting in decreased heart rate, body length, elicited movement and spontaneous movement, including the number of times ZFEs spontaneously moved during the assessment time of one minute. MeHg exposure in ZFEs had no significant effect on mortality rate, hatching rate, yolk sac area,

heart volume, ventricle thickness, and pericardial cavity volume, as well as clustering of acetylcholine receptors (AChRs) and presynaptic vesicle aggregates at the NMJ.

This study has confirmed previous reports in the literature that MeHg exposure has adverse effects on the general development of ZFEs. MeHg exposure also had adverse effects on heart development as well as skeletal muscle development, which adversely effected movement. Exposure to 24 hours of low concentrations of MeHg is likely to result in functional deficits that are not reflected in obvious morphologic deficits.

DEDICATION

This thesis is dedicated to my parents whom have always provided me with love and support. I have learned so much by watching and learning from you both. You have made me the person I am today, and I can't express to you how lucky and happy I am to live my life with such beautiful individuals. You make everything in life wonderful. I love you both so very much! I will pass down your lessons and wisdom on to my future children and they too will know how beautiful their grandparents are.

This thesis is also dedicated to the love of my life. You have made my life so rich that I might get diabetes! We have been through so much together and can't think of anyone else I'd rather spend my life with. You're a magnificent being and I can't put into words how beautiful you truly are. You bring out the absolute best in me and I'm so thankful for the first day I laid eyes on you.

ACKNOWLEDGEMENTS

I would like to thank my committee chair, Dr. Louise Abbott, and my committee members, Dr. Mark Zoran, and Dr. Michelle Pine, for their guidance and support throughout the course of this research.

I would like to thank Lin Bustamante and Chaitali Mukherjee at the VIBS histology laboratory. Thanks also goes to Dr. Bruce Riley's lab especially Jennifer Dong for provided assistance with the zebrafish embryos. I would also like to use this opportunity to acknowledge the advice and help from Dr. Jane Welsh and Dr. Roula Mouneimne. A very special thanks goes to Dr. Fikru Nigussie and Dr. Alice Villalobos for always being available when I needed advice, assistance and support. Both of you have definitely made my experience much more enjoyable. I also want to extend my gratitude to my student workers Kara Eichelkraut, Eric Johnson, Jessica Vanschuyver, Jasmine McGoldrick, and David Terry, whom worked diligently by my side.

Finally, thanks to my fantastic parents for their encouragement and to my boyfriend and our daughter for their support, patience and love.

NOMENCLATURE

AChR	Acetylcholine receptor
CNS	Central nervous system
H&E	Hematoxylin and Eosin
Hg	Mercury
hpf	Hours post fertilization
IHC	Immunohistochemistry
MeHg	Methylmercury
NMJ	Neuromuscular junction
NT	Neurotransmitter
ppb	Parts per billion
ROS	Reactive oxygen species
ZFE	Zebrafish embryo

TABLE OF CONTENTS

Page

LIST OF FIGURES

Page

LIST OF TABLES

Page

I. INTRODUCTION

Methylmercury as a neurotoxicant

Mercury has three major forms in which it occurs: elemental mercury, inorganic mercury and organic mercury (Korbas et al., 2011, Hassan et al., 2012). Elemental mercury (Hg) is a heavy metal that is converted into methylmercury (MeHg) by sulfate-reducing bacteria located in both fresh and saltwater sources (Kaschak et al., 2014). These bacteria add a methyl group to Hg in a process referred to as biotransformation (Klášterská and Ramel, 1978, Hassan et al., 2012, Kaschak et al., 2014). Hg occurs naturally in the environment where it is released into local water sources through erosion of minerals in rocks and soil along with volcanic eruptions; this accounts for 30% of Hg introduced into the environment. 70% of Hg is introduced into the local water source through runoff from industrial processing plants and mercury-containing fungicides, while Hg vapors are introduced into the atmosphere through coal-fired electrical power plants and waste incineration plants (Trasande et al., 2005). MeHg is highly lipophilic and when absorbed by aquatic plankton, which forms the base for the food chain thus allowing MeHg to enter the food chain. MeHg readily accumulates in the tissues of small organisms that eat plankton or directly absorb MeHg from the water and then larger organisms eat the smaller ones, causing MeHg to collect in these organisms. This process of MeHg transfer in the food chain is called bioaccumulation (Halbach, 1990, Mergler et al., 2007, Hassan et al., 2012). MeHg has been shown to bind to proteins as

well as amino acids, particularly cysteine residues, which contain sulfhydryl groups that are essential components of many different tissues, and specifically muscle (Halbach, 1990, Mergler et al., 2007, Li et al., 2010).

Small fish eat organisms containing MeHg and then they are eaten by larger fish and so on. Fish that live a long time and grow to very large sizes will have the most MeHg present in their tissues due to bioaccumulation through the food chain (Klášterská and Ramel, 1978). Large, long-lived predatory fish include swordfish, tuna, king mackerel and shark, which are prime food sources for humans (Mergler et al., 2007, Hassan et al., 2012). When we consume these fish we are also ingesting MeHg contained in the muscle tissue, which is of significant concern especially for pregnant mothers. Consumption of contaminated fish is the most common way individuals are exposed to MeHg but seed grain can also be a source of exposure when MeHg is used as a fungicide; the use of MeHg as a fungicide is most common in other parts of the world such as Iraq and China (Klášterská and Ramel, 1978, Myers et al., 2003).

MeHg is most easily absorbed through the digestive tract where about 95% is absorbed. MeHg is distributed throughout the entire body in about 30 to 40 hours, where 5% remains in the blood compartments bound to proteins within plasma (Li et al., 2010). The other 5% will remain in various organs, specifically the brain. Once MeHg enters the body it is either demethylated or partly demethylated (Vahter et al., 1994). Therefore, elemental forms and inorganic forms of Hg are present in the body where it can persist for long periods of time, potentially the life of the organism (Vahter et al., 1994, Philbert et al., 2000, Korbas et al., 2011). Approximately 90% of MeHg is excreted through feces

(Li et al., 2010). Since MeHg enters the bloodstream after it is absorbed from the digestive tract, this means that an unborn child can be exposed to MeHg because it can easily cross the placenta (Chen et al., 1979, Myers et al., 2003). MeHg has also been shown to pass into a nursing mother's breast milk (Davidson et al., 2004). For these reasons the United States Environmental Protection Agency (EPA) recommended that pregnant women limit their fish intake to two 6-ounce servings per week and avoid consumption of fish species that may be high in mercury (Oken et al., 2008).

MeHg has been shown to have adverse effects on the central nervous system (CNS), which is especially harmful to a growing fetus. An incident in Minamata, Japan during the early 1950s initiated the investigation of MeHg as a neurotoxicant (Harada, 1995). Chisso Minamata industrial plant that produced chemical fertilizers, synthetic resins, plasticizers, and industrial chemicals had discharged large quantities of waste directly into the Minamata Bay, which contaminated the bay along with the residents' main food source (Harada, 1995). Soon after strange behavior was witnessed such as fish rotating, floating belly up to the surface, birds falling while in flight, cats convulsing and unable to walk and often died (Harada, 1995).

Acute MeHg poisoning in adults results in visual and hearing impairment, olfactory and gustatory disturbances, cerebellar ataxia, somatosensory disturbances and psychiatric symptomatology. Children born to mothers whom consumed contaminated fish during their pregnancy showed symptoms such as mental retardation, decrease in primitive reflexes, cerebellar ataxia, disturbances in physical development and nutrition, and deformity of limbs just to name a few (Harada, 1995). Findings demonstrated

damage to the CNS especially in the cerebral cortex and cerebellar cortex (Harada, 1995). The cerebellum plays a critical role in motor control where MeHg will specifically target cerebellar granules cells. These cells are essential for relaying information from the white matter to multiple cells, most importantly the Purkinje cells, within the molecular cell layer (Patel and Reynolds, 2013). The peripheral nervous system (PNS) demonstrated destruction and demyelination of the dorsal root of the spinal cord (Harada, 1995, Ekino et al., 2007).

A cohort study of the human population in the Faroe Islands also found that prenatal exposure to MeHg, through the consumption of fish and whale tissues, was associated with neurodevelopmental deficits in children such as poorer performance on tests of language and intelligence (Myers et al., 2003). A cohort study conducted in the Republic of Seychelles also focused on prenatal exposure to MeHg but found little effect associated with MeHg exposure. This is a controversial finding considering that 85% of the Seychelles population consumes marine fish daily (Davidson et al., 1998). Many researchers have proposed various reasons as to why the Seychelles cohort demonstrated little effect resulting from MeHg exposure. One compelling argument is that the seafood consumed in the Republic of Seychelles had a lower mean concentration of MeHg at 0.3 µg/g, which is similar concentrations in fish consumed in the USA. Mean concentration of MeHg in whale meat in the Faroe Islands is 1.6 µg/g which is 4 times higher (Myers et al., 2003).

Although, the effects of MeHg at high concentrations should be investigated lower concentrations are also of importance, particularly when considering the

concentrations that the US population would normally encounter. According to the US Food and Drug Administration (FDA) the current Hg concentrations in various fish species is lower than 1 ppm. Since the concentrations encountered in the Seychelles cohort study are similar to concentrations in fish consumed in the USA, this study allows for a more accurate comparison to be made between these populations.

When considering symptoms demonstrated by individuals with MeHg poisoning it is obvious that MeHg exposure adversely affects the nervous system. It has been demonstrated that MeHg accumulates in astrocytes, which results in swelling of astrocytes; to correct for this swelling astrocytes release excitatory amino acids such as glutamate and this could result in neuronal impairment, injury and death (Aschner et al., 2000). Another target for MeHg is glutamate; glutamate is an excitatory neurotransmitter (NT). This NT must be maintained at a specific level at the synaptic cleft to prevent excitotoxicity, which leads to increased Na^{+} and Ca^{2+} influx into neurons via over activation of N-methyl D-aspartate type glutamate receptors present on post synaptic membranes (Allen et al., 2001, Choi et al., 2008). This intracellular increase in Ca^{2+} levels is associated with oxidative stress and toxic insult to neurons (Allen et al., 2001, Farina et al., 2011).

Reactive oxygen species (ROS) are produced naturally in the body through processes such as aerobic respiration, where ROS are a byproduct of mitochondria. MeHg exposure may change mitochondrial morphology, possibly disrupting the electron transport chain (Bellum et al., 2007, Farina et al., 2011). The brain demands large amounts of energy production, which could lead to large amounts of ROS byproducts. A

study done by Bellum et al. 2007 measured ROS production in cerebellar granule cells of MeHg exposed mouse pups, and demonstrated an increase in ROS production associated with MeHg exposure. A study using cultured cerebellar granule neurons demonstrated that the formation of specific ROS can lead to necrosis and apoptosis of these neurons (Valencia and Morán, 2004). MeHg exposure and an increase in ROS could adversely affect the developing nervous system.

In humans, MeHg was shown to promote production of free radicals by inactivating antioxidant properties of glutathione, catalase and superoxide dismutase (Guallar et al., 2002). These antioxidants are crucial for protecting cells against oxidative stress; inactivating these antioxidants causes increased ROS. Lipid peroxidation is the process of degrading lipids via oxidation. Therefore, an increase in oxidative stress can trigger an increase in lipid peroxidation. A study conducted on neuronal tissues of MeHg treated adult rats demonstrated an increase in the rate of lipid peroxidation along with a decrease in DNA as well as RNA content in all brain parts but was highest in the cerebellum (Zahir et al., 2006).

Due to its affinity for sulfhydryl groups, MeHg has also been demonstrated to combine covalently with plasma cholinesterase, which leads to inhibition of plasma cholinersterase (Hastings et al., 1975). Plasma cholinesterase is similar to acetylcholinesterase, which suggests a similar mechanism of action by MeHg on acetylcholinesterase may be possible. Acetylcholinesterase is present at synaptic clefts at the neuromuscular junction (NMJ), neuronal synapses and membranes of red blood cells. Inhibition of acetylcholinesterase is problematic since it is an essential enzyme in

catalyzing acetylcholine, which allows for neurons and effector organs (including muscle) to return to their resting state. Neurons and muscle cells not allowed to return to their resting state can lead to excitotoxicity.

Studies have shown that MeHg exposure can lead to coronary artery and carotid atherosclerosis, elevate blood pressure, and myocardial infarction in humans (Guallar et al., 2002, Choi et al., 2008). A study conducted by Halbach 1990 demonstrated that due to the lipophilic nature of MeHg it binds to thiol groups within the membrane of cardiac cells resulting in negative inotropic effect in heart tissues of guinea pigs. A negative inotropic effect on the heart reduces the force of muscle contraction resulting in a decrease in heart rate. These reports just mentioned result in some controversy, since the study on humans suggests an increase in heart rate while the guinea pig study reported a decrease in heart rate. The effect of MeHg exposure on heart function warrants further investigation.

Pericardial cavity volume has not been assessed extensively in the published literature, but one study conducted on hamsters demonstrated pericardial cavity distention after prenatal exposure to inorganic mercury (Gale, 1981). Edema of the pericardial cavity or pericardial effusion occurs when too much serous fluid is being produced. Pericardial effusion has been associated with various impairments in the cardiovascular system.

General zebrafish development

By using zebrafish embryos (*Danio rerio*) as our animal model we will be able to investigate mechanisms by which MeHg causes neurodevelopmental and anatomical defects. Zebrafish embryos (ZFEs) are an excellent animal model since we can observe the embryo throughout its development due to the presence of a clear chorion (protective covering), the transparency of the embryo, rapid ex utero development and the possibility of direct delivery of MeHg to the developing ZFE (Sylvain et al., 2011, Hassan et al., 2012). To understand mechanisms underlying MeHg toxicity we first must understand normal ZFE development.

Periods of early development include: zygote, cleavage, blastula, gastrula, segmentation, pharyngula, hatching and early larva (See Table 1, taken from Kimmel et al., 1995). During early development, the age of the embryo is defined as the number of hours that have passed since initial fertilization (hours post fertilization or hpf). The following description of normal ZFE development is summarized from Kimmel et al., 1995 (Kimmel et al., 1995). After fertilization the zygote undergoes multiple cell division or cleavages. The cleavage period is characterized by rapid mitotic cell division in the blastodisc, which is a dome of cytoplasm that is separate from the yolk mass and located toward the animal pole of the early developing embryo. The cell layer that forms on the superficial surface of the blastodisc is referred to as the layer of enveloping cells. The next stage is the blastula period where the ZFE forms a yoke syncytial layer (YSL), and epiboly begins. The YSL is formed via some cells collapsing and depositing their

nuclei and cytoplasm into the cytoplasm of the yolk mass. The nuclei of these collapsing cells line up in a single row along the blastodisc margin. Epiboly is the thinning and spreading of the YSL and blastodisc over the yolk mass. Epiboly is described as percent-epiboly, which indicates how much or percentage of the yolk mass that is covered by the blastodisc. As the YSL and blastodisc spread, the enveloping cell layer (EVL) is pulled along with the YSL since the edge of the EVL is connected to the YSL; the yolk mass starts to bulge into the blastodisc. Once epiboly is at 30% the blastodisc is called the blastoderm, which consists of the EVL and a deeper multicellular layer (DEL) (Kimmel et al., 1995, Carvalho and Heisenberg, 2010).

As epiboly continues into the gastrulation period, a germ ring (5 hpf) forms, which is located around the blastoderm rim. Since epiboly is not complete at the time the germ ring forms, the rim or margins of the blastoderm are visible. The rim is where the germ ring is formed due to involution which is the process by the mesoderm and endoderm progenitors (hypoblast) from the DEL folds inward and back upon themselves, while the ectoderm progenitors (epiblast) remain on the exterior of the embryo (Carvalho and Heisenberg, 2010). Ectoderm eventually forms skin, nervous system, neural crest and sensory placodes; mesoderm gives rise to muscles and bones; and endoderm forms most of the internal organs (Kimmel et al., 1995, Stickney et al., 2000).

Table 1. Periods of early development. Table taken from Kimmel, 1995.

Period	h	Description
Zygote	0	The newly fertilized egg through the completion of the first zygotic cell cycle
Cleavage	¾	Cell cycles 2 through 7 occur rapidly and synchronously
Blastula	2¼	Rapid, metasynchronous cell cycles (8, 9) give way to lengthened, asynchronous ones at the midblastula transition; epiboly then begins
Gastrula	5¼	Morphogenetic movements of involution, convergence, and extension form the epiblast, hypoblast, and embryonic axis; through the end of epiboly
Segmentation	10	Somites, pharyngeal arch primordia, and neuromeres develop; primary organogenesis; earliest movements; the tail appears
Pharyngula	24	Phylotypic-stage embryo; body axis straightens from its early curvature about the yolk sac; circulation, pigmentation, and fins begin development
Hatching	48	Completion of rapid morphogenesis of primary organ systems; cartilage development in head and pectoral fin; hatching occurs asynchronously
Early larva	72	Swim bladder inflates; food-seeking and active avoidance behaviors

Next, convergence of cells takes place, which is the movement of the deep cells toward the dorsal side of the embryo. Convergence is first observed or noted when an embryonic shield is seen, which is a thickened portion of both the epiblast and hypoblast. The embryonic shield is one of the first signs of dorsoventral polarity in ZFEs; the embryonic shield will then elongate along the anterior-posterior axis (Shih and Fraser, 1996). The dorsal epiblast thickens anteriorly to begin formation of the neural

plate (Kimmel et al., 1995). Toward the end of the gastrulation period (10 hpf) a swelling is observed at the posterior end of the anterior-posterior axis of the embryo called the tail bud. The neural plate formation is now along the entire axis of the embryo. Epiboly is complete at the end of the gastrula period where the YSL, EVL and blastoderm engulf the entire yolk mass.

During the segmentation period (10-24 hpf) the neural plate elongates and forms a neural groove and neural folds. The neural groove is a depressed mid-region of the embryonic shield; next, neural folds form, which are elevated folds on either side of the neural groove. These folds fuse to form a neural rod, which will eventually hollow out to form the neural tube (19 hpf); the neural tube is the primordium of the CNS (Schmidt et al., 2013). Another tube that lies ventral to the neural tube is distinguishable and it is the notochord. The notochord is a rod-shaped tube that is needed for axial body support similar to the vertebral column of higher vertebrates. The yolk mass constricts in the posterior region of the ZFE, where the tail bud ends. This narrow, posterior elongation of the yolk sac, formally known as the yolk mass, is called the yolk extension. The tail bud, which was curled around the original vegetal pole, and growing towards the head increases in length resulting in the straightening of the tail, where it protrudes away from the body. The combination of yolk mass constriction and lengthening of the tail, results in the straightening of the posterior trunk. Although the tail of the ZFE is in the process of straightening the ZFE is still curled within its chorion. At 19 hpf the brain is distinguishable, including its ventricles. Weak muscle contractions or spontaneous movement of the embryo can be seen at 22 hpf (Kimmel et al., 1995).

Somites develop during the segmentation period; the first somite can be seen at about 10 hpf where anterior somites form first and develop sequentially down towards the tail. Somites are undifferentiated mesodermal component of an early trunk or tail segment (Kimmel et al., 1995). Somites contain undifferentiated mesodermal components that eventually differentiated into sclerotomes, myotomes and possibly dermatomes (Kimmel et al., 1995, Stickney et al., 2000). Sclerotomes give rise to vertebral cartilage that migrate around and envelop the neural tube and notochord. Myotomes give rise to muscle and are the predominate cell type in the somite. It is unclear whether ZFEs have dermatomes, which give rise to the dermis of the skin. Waterman (1969) identified cells on the surface of myotomes that he called external cells, but whether these cells constitute dermatomes is still unclear (Waterman, 1969, Stickney et al., 2000). Dorsal and ventral halves of each somite are separated by connective tissue called the horizontal myoseptum while adjacent somites are separated by a vertical myoseptum. These myosepta, along with the notochord, are attachment sites for skeletal muscle fibers (Bassett and Currie, 2003). One can also observe initial formation of the primary organs, including the heart, at the segamentation stage of development (Kimmel et al., 1995).

The pharyngula period (24-48 hpf) is characterized by development of pharyngeal arches. There are seven pharyngeal arches where the first two arches (mandibular and hyoid arches) form the jaws and operculum (a hard bony flap covering the gill slits), and the remaining arches (branchial arches) form the gills (Kimmel et al., 1995). Pigment formation is now seen at 24 hpf, first in the cells of the pigmented retinal

epithelium of the developing eye, then in melanophores in the skin. The melanophores will eventually migrate to define the typical striped pattern of the body, giving zebrafish their name. The heart started to form at about 18 hpf, with fusion of the left and right cardiac precursors. Just before the pharyngula period the heart starts to beat in a disorganized matter, including an irregular pattern of beating and no synchronized direction in the beats. The circulatory system becomes a closed system at the pharyngula stage where blood begins to circulate slowly. Spontaneous movement of the tail, which started at 22 hpf peaks with respect to frequency and then begins to decrease during this developmental period (Kimmel et al., 1995).

During the hatching period (48-72 hpf) the embryo continues to grow and will hatching from its chorion as some time during this stage. Many organs undergo significant development, including rapidly developing jaws, gills and fins. Due to utilization of the yolk as an energy source during development the yolk sac is smaller, which allows for greater visibility of the pericardial cavity and heart. At this stage the heart beats strongly, in a synchronized manner and a full circulatory system present. At 72 hpf the mouth is well developed and as is the digestive tract. The hatched ZFE has completed most of its morphogenesis.

Once hatched the ZFE enters the early larva stage, and continues to grow larger. Inflation of the swim bladder occurs at approximately 72 hpf and the larva becomes more active, including the ability to exhibit avoidance behaviors (Kimmel et al., 1995).

Zebrafish central nervous system development

Using ZFEs as an animal model is advantageous since the development of the CNS is well understood (Kimmel et al., 1995, Drapeau et al., 2002). At the beginning of the segmentation period (16 hpf), ten swellings (neuromeres) form in the neural tube; the first three correspond to the diencephalon, telencephalon and the mesencephalon (Kimmel et al., 1995). The diencephalon gives rise to the thalamus, hypothalamus, posterior portion of pituitary gland, and pineal gland. The telencephalon gives rise to the cerebral cortex, basal ganglia, corpus striatum and olfactory bulb. The mesencephalon gives rise to the superior colliculus and inferior colliculus. The remaining seven neuromeres (rhombomeres) subdivide the hindbrain (See Figure 1, taken from Kimmel et al., 1995); the hindbrain gives rise to pons, cerebellum and medulla. Just before the pharyngula period the cerebellum is recognizable and the brain has five distinct lobes (Kimmel et al., 1995).

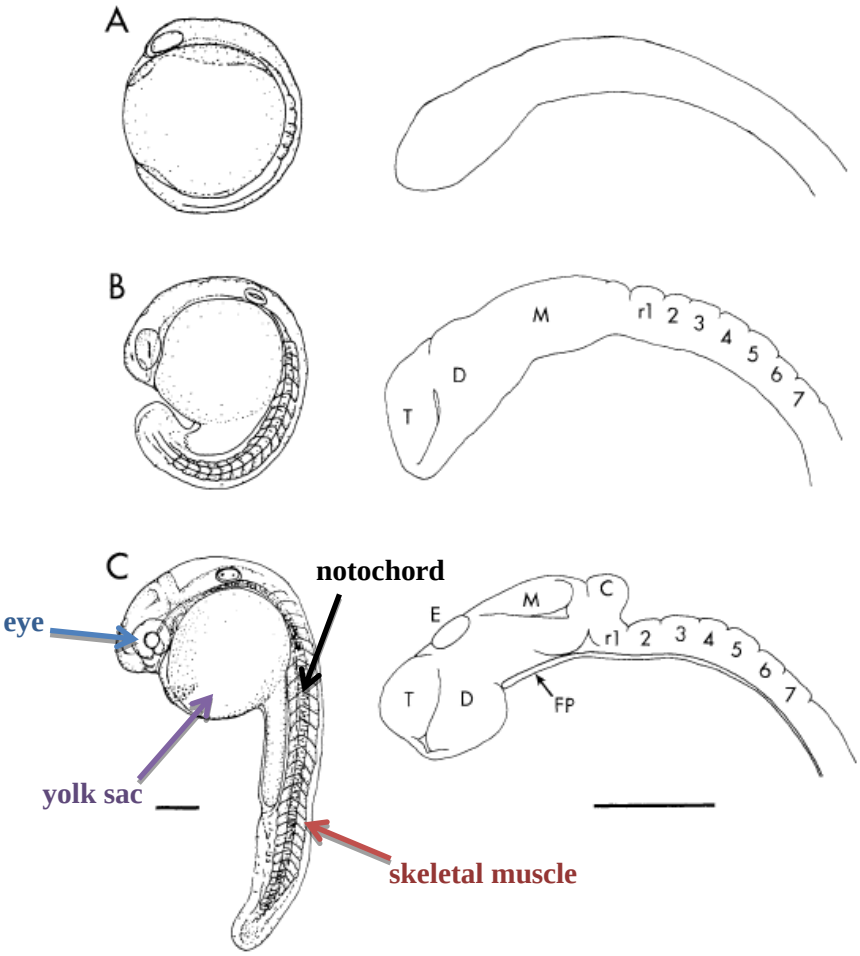

Figure 1. Formation of the brain during the segmentation period. A) No subdivision at 12 hpf. B) At 18 hpf we have ten neuromeres. C) At 24 hpf. T = telencephalon, D = diencephalon, M = mesencephalon, FP = floor plate, C = cerebellum, E = epiphysis, r1-r7 = seven hindbrain rhombomeres, scale bar = 200 µm. (Modified from Kimmel, 1995).

The general organization of the neural tube is such that sensory neurons form in the dorsal region, motor neurons form in the ventral region and interneurons occupy the intermediate region (Blader and Strähle, 2000). After the neural tube has formed during the segmentation period, at approximately 15 hpf the first neurons begin to differentiate, which are called primary neurons. These primary neurons, both motor and sensory, develop large cell bodies and extend their axons between different regions of the neural tube such as between the hindbrain and spinal cord or between neural tube and periphery (in the case of sensory and motor neurons) (Kimmel et al., 1995).

The ZFE initially develops three longitudinal axonal tracts in the spinal cord that form in the following sequence: dorsal longitudinal fasciculus (DLF), ventral longitudinal fasciculus (VLF), and medial longitudinal fasciculus (MLF) (Drapeau et al., 2002). Rohon-Beard (RB) sensory neurons, located at the dorsal aspect of the spinal cord, pioneer the DLF by extending axons both rostrally and caudally at 15 hpf. At 16 hpf peripheral sensory axons, RB sensory neurons, extend to the skin while its centrally located axons form the DLF along the wall of the spinal cord. Dorsal longitudinal ascending (DoLA) interneurons also extend into the DLF, at 17 hpf, which sends axons rostrally to the hindbrain by 26 hpf. Ventral longitudinal descending (VeLD) interneurons extend axons caudally pioneering the VLF. Caudally directed axon (IC) pioneers the MLF by extending axons caudally from the caudal hindbrain and rostral spinal cord (See Figure 2; Kimmel et al., 1995, Drapeau et al., 2002).

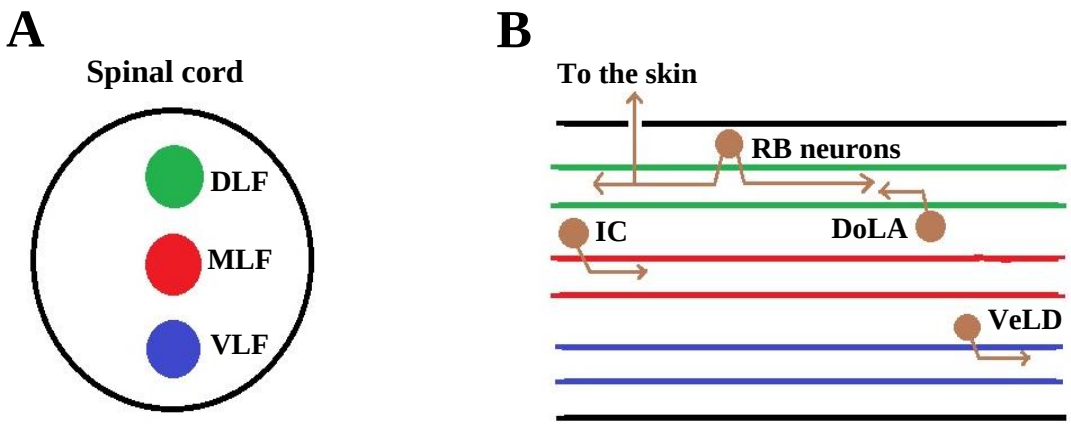

Figure 2. Three longitudinal axonal tracts. A) Cross section through the spinal cord and three longitudinal axonal tracts. DLF = dorsal longitudinal fasciculus (green), VLF = ventral longitudinal fasciculus (blue), MLF = medial longitudinal fasciculus (red). B) Sagittal section through the spinal cord and three longitudinal axonal tracts. Left side of the image is the rostral aspect of ZFE, top of image is the dorsal aspect. RB neurons = Rohon-Beard sensory neurons, DoLA = dorsal longitudinal ascending interneurons, VeLD = ventral longitudinal decending interneurons, IC = caudally directed axons. Brown arrows indicate axonal growth in a particular direct.

Three primary motor neurons are present along each side of the spinal cord segments, which correlate with each of the myotome segments. The first primary motor neuron extends its axon out of the spinal cord (premature ventral root) and grows ventrally within the mytome at about 17 hpf. The second primary motor neuron extends its axon into the middle of the myotome; the third primary motor neuron extends its axon dorsally within the myotome. The first wave of motor neurons comes in contact with the pioneer muscles first before extending out into the myotome (Stickney et al., 2000, Drapeau et al., 2002). Pioneer muscles are adaxial mesoderm cells that are essential in providing signals for motor neuron pathway choice and will be talked about more in depth in the following section. At 26 hpf a second wave of motor neurons, secondary motor neurons, send axons out of the spinal cord through the ventral root and branch into the muscle mass. At 72 hpf most of the motor neurons have innervated muscle cells, evidence for which can be seen by locomotor responses by the ZFE (Kimmel et al., 1995).

Weak muscle contraction or spontaneous movement can be seen once the primary motor neurons innervate myotomes. Skeletal muscle in ZFEs is polyneuronally innervated by primary and secondary motor neurons (Drapeau et al., 2002, Sylvain et al., 2011). These motor neurons extend axons to the developing muscle cells and the first neuromuscular junctions (NMJ) are formed where they elicit contraction (Kimmel et al., 1995). NMJs are the sites where motor neurons synapse with a muscle cell. Motor neurons send signals from the CNS to the muscle cell via neurotransmitters (NT). NTs are endogenous chemicals signals sent across a synaptic cleft, the gap between neuron

and muscle. Acetylcholine (ACh) is an excitatory NT released from axon terminals at NMJs, via pre-synaptic vesicles. ACh binds to acetylcholine receptors (AChRs) present on the muscle cell, which, when stimulated, result in a muscle contraction. Around the time that primary motor neurons innervate the muscles, clusters of AChRs are also first detected. This clustering of AChRs occurs a few hours after contact has been made between the axon terminals and muscle cells (Nguyen et al., 1999). Signals from the CNS travel through two general categories or subtypes of motor neurons: upper motor neurons (UMNs) and lower motor neurons (LMNs). UMNs are located within the brain and must synapse with LMNs to send signals to skeletal muscle. LMN are found in cranial and spinal nerves.

Zebrafish skeletal muscle development

ZFEs have two types of muscle fibers: slow tonic fibers, which are located directly underneath skin, and fast twitch fibers, which are located deep to the slow tonic fibers (See Figure 3, taken from Devoto et al., 1996). The slow fibers are only active during slow swimming episodes while fast fibers are active during fast swimming episodes (Drapeau et al., 2002, Sylvain et al., 2011).

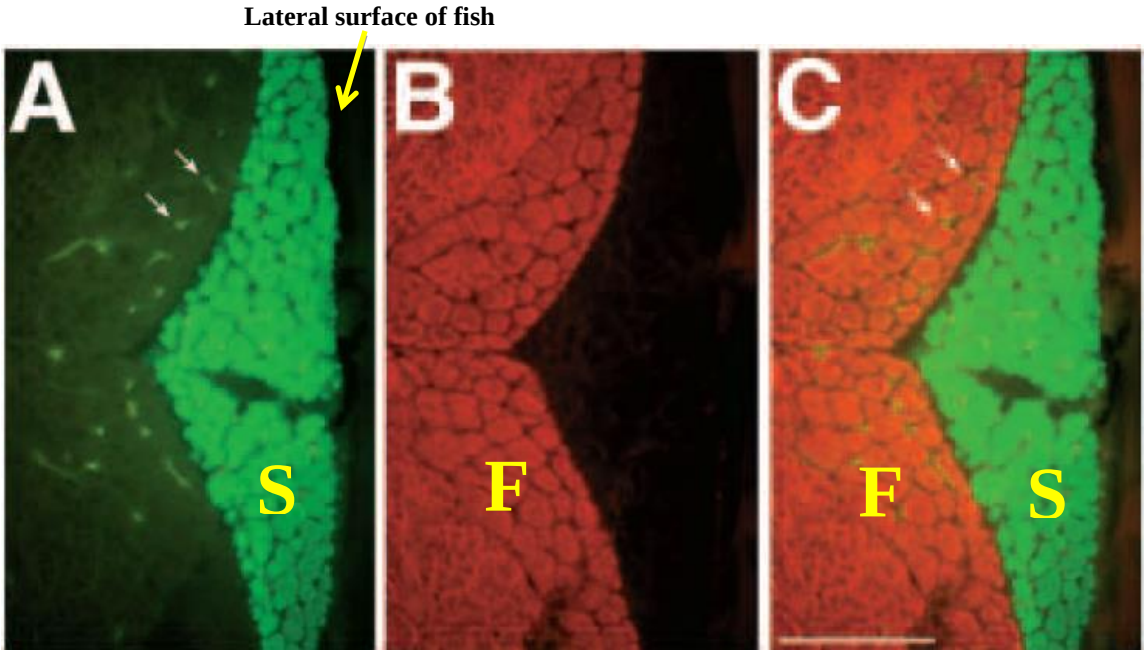

Figure 3. Slow and fast muscle fibers distinguished by immunolabeling. A) S58 (green) recognizes only slow muscle fibers (S). B) 12/101 (red) recognizes fast muscle fibers (F). C) S58 and 12/101 labeling. These are transverse sections of a 32 dpf ZF; dorsal is located at the top of each photograph. White arrows = non-specific fluorescence is present within blood vessels in all muscle regions, Scale bar = 100 µm (Modified from Devoto, 1996).

During the gastrula period, before the first somite is distinguishable, undifferentiated mesoderm located on both sides of the neural tube is called paraxial mesoderm. Paraxial mesoderm cells differentiate, by 16 hpf, into adaxial mesoderm and these cells will be signaled to migrate to the lateral somite periphery. The first somite forms at 10 hpf. The adaxial mesoderm cells differentiate into slow tonic fibers. A small population of adaxial mesoderm remains in its medial location near the notochord and these cells migrate dorsally and ventrally. The medially located adaxial mesoderm cells become pioneer muscle fibers that elongate and radiate laterally through the somite at the level of the future horizontal myoseptum (Devoto et al., 1996, Drapeau et al., 2002, Bassett and Currie, 2003, Sylvain et al., 2011). Pioneer muscles cells are considered to be essential in providing signals for motor neuron pathway choice, but they do not appear to be needed for axon guidance (Melançon et al., 1997, Stickney et al., 2000). Lateral to the paraxial mesoderm is the lateral paraxial mesoderm, which differentiates into lateral presomatic muscle precursor cells. These muscle cells give rise to fast twitch fibers, which forms the bulk of the skeletal muscle. This differentiation process occurs while the adaxial cells migrate laterally pass them (See Figure 4, taken from Stickney et al., 2000).

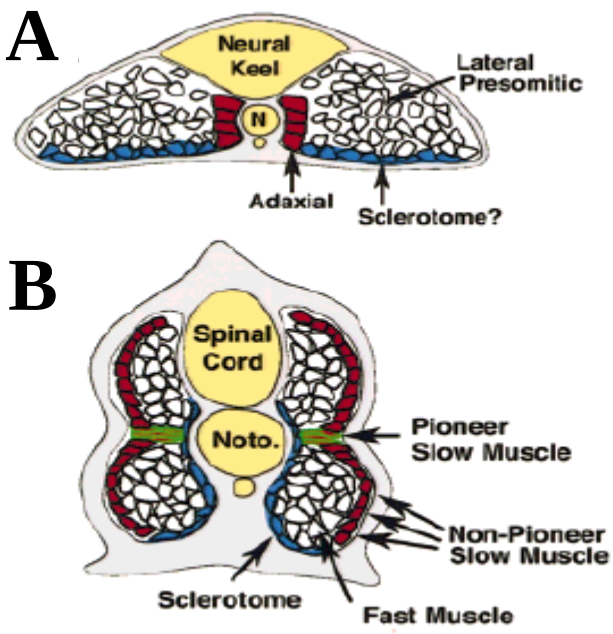

Figure 4. Zebrafish somite. Demonstrates adaxial mesoderm (labeled Adaxial), sclerotome, pioneer slow muscle fibers (previously adaxial mesoderm in diagram A) and lateral presomitic muscle (from lateral presomitic mesoderm) distribution (Modified from Stickney, 2000).

Countless events occur during development, but one very important event is development of the heart. The zebrafish heart, which is a single tube, consists of four regions: sinus venosus, atrium, ventricle, and bulbus arteriosus (Stainier et al., 1993, Hu et al., 2000). The heart pumps deoxygenated blood out of the bulbus arteriosus to the ventral aorta, which leads to the gill arches where oxygenation occurs and then the blood is distributed throughout the body (Hu et al., 2000). At 15 hpf cardiac precursors move toward the lateral plate mesoderm where it generates a pair of tubular primordia, one on

each side of the midline. The tubular primordia move toward the midline and fuse, forming a single heart tube by 21 hpf. The single heart tube consists of endocardial cells lining the central lumen and myocardial cells peripherally (Stainier et al., 1993, Keßler et al., 2012). The heart tube becomes elongated by 24-26 hpf when it begins to contract, and at 42 hpf the heart beats at about 180 beats per minute (Keßler et al., 2012). At about 48 hpf the heart has the basic architecture found in the adult fish heart (See Figure 5, taken from KeBler et al., 2012), but the heart will continue to mature further as the ZFE develops (Heideman et al., 2005). At 48 hpf, all four segments are smooth-walled and the myocardium is about one cell thick except for the ventricle which has two to three cell layers. The heart is lined with endocardium and is separated from the myocardium by a layer of cardiac jelly in the atrium and bulbus arteriosus. The heart is covered with epicardium and is enclosed in the pericardial cavity. There are no valves separating each segment at 48 hpf (Hu et al., 2000).

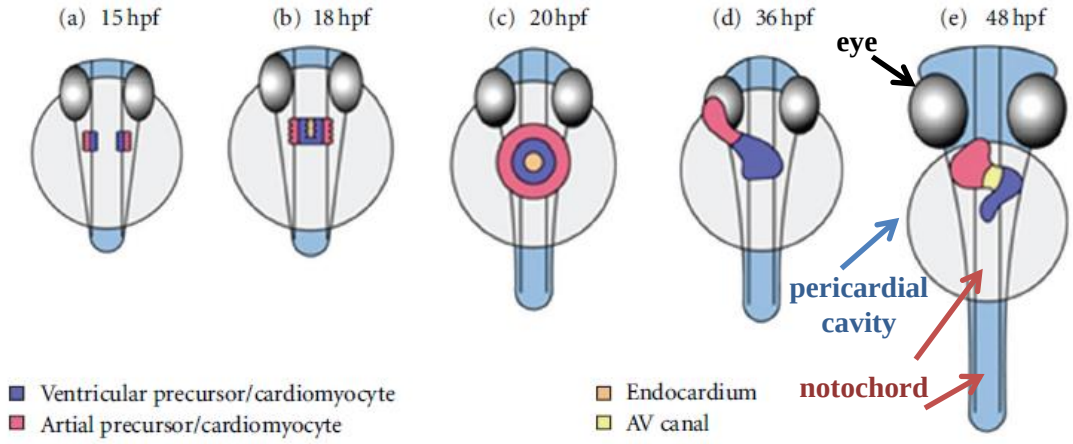

Figure 5. Stages of heart development in ZFEs in ventral view. Modified from KeBler, 2012.

Rationale for this study

Zebrafish embryos (ZFEs) are an animal model that can be used to assess the effects of MeHg exposure. The use of ZFEs in this study, allowed us to investigate mechanisms of action of this neurotoxicant.

MeHg concentrations are usually expressed as parts per million, (ppm), which is mg/L or parts per billion (ppb), which is µg/L. A study by Hassan et al. 2012 demonstrated that ZFEs exposed to 200 ppb MeHg for 24 hours resulted in 83.3% mortality rate while lower concentrations of MeHg (5, 10 and 50 ppb) did not show significant mortality rates. A low mortality rate among ZFE groups exposed to MeHg is ideal for this study to investigate neurotoxic effects of MeHg exposure on ZFE development. MeHg exposure in ZFEs also results in defects of the median finfold, tail

fin primordium and flexure of the posterior tail region (Samson and Shenker, 2000, Yang et al., 2010). These defects could adversely affect movement of the ZFE, specifically spontaneous and elicited movement.

Since one of the most characteristic features of exposure to high concentrations of MeHg results in kinked tails and abnormal/disorganized skeletal muscle (See Figure 6), ZFEs may be less effective at breaking through the chorion (Yang et al., 2010). High concentrations of MeHg exposure have been shown to delay or inhibit ZFEs' ability to hatch from the chorion (Hassan et al., 2012). ZFEs typically start hatching around 40 hours post fertilization (hpf) while complete hatching should occur by 72 hpf (Kimmel et al., 1995). Delayed development could result in alterations in body length and yolk sac area of experimental ZFEs as well as affect other developmental processes, including heart development.

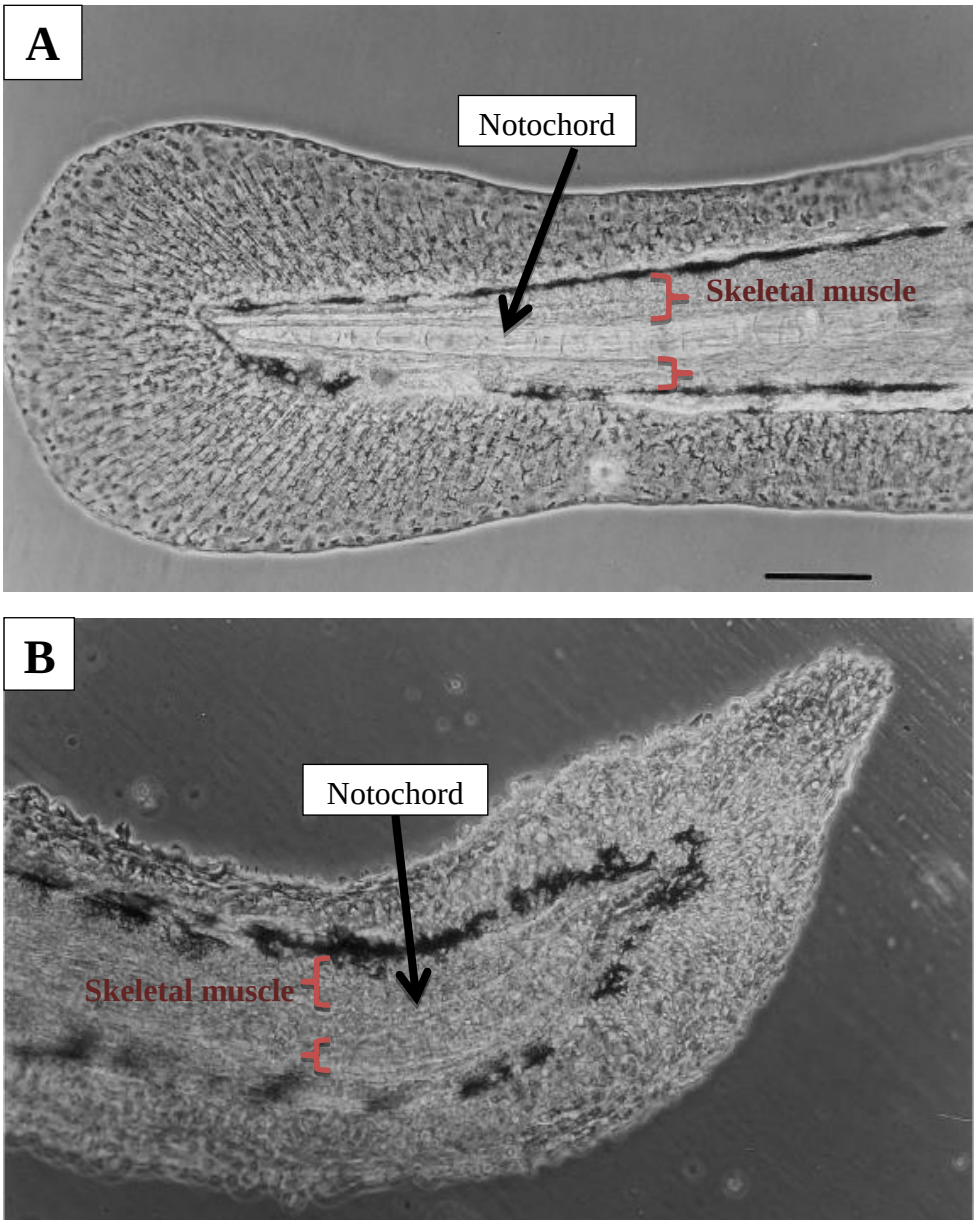

Figure 6. Morphological defects in the median finfold and posterior tail region of newly hatched ZFE after exposure to MeHg. A) Normal development. B) Severe flexure of the entire posterior-most tail region (Modified from Samson, 2000).

The purpose of this study is to better understand the neurotoxic effects of MeHg on ZFE development, where we investigated overall embryo development, heart development and neuromuscular junction (NMJ) development. The aims of this thesis were to use ZFEs as our animal model to determine developmental effects of MeHg exposure at different concentrations on: (1) heart development and (2) NMJ development.

The overall hypothesis for this study is that MeHg exposure has adverse effects on muscle development, specifically heart and skeletal muscle. We hypothesize that MeHg exposure will result in abnormalities of cardiac muscle affecting heart rate, heart volume, ventricle thickness and pericardial cavity volume. We also hypothesize that MeHg exposure will result in abnormal of the skeletal muscle development, particularly at the NMJ, resulting in abnormal movement.

First, we determined the general developmental effects of MeHg on mortality rate, hatching rate, body length and yolk sac area. Exposure to high concentrations of MeHg can lead to high mortality rates, so to investigate developmental effects of MeHg exposure we used relatively low MeHg concentrations (Hassan et al., 2012). We used three groups of ZFEs: controls, 10 ppb MeHg exposure and 50 ppb MeHg exposure.

Second, we determined effects of MeHg exposure on heart development by investigating heart volume, ventricle thickness and pericardial volume. It has been reported that MeHg exposure may lead to heart disease in humans and edema of the pericardial cavity in hamsters. We hypothesized that embryos exposed to MeHg would demonstrate a higher heart rate relative to controls. We also hypothesized that heart

volume in MeHg exposed ZFEs would be smaller and ventricle thickness would be increased relative to control ZFEs. We also hypothesized that pericardial cavity volume would be increased in MeHg exposed ZFEs compared to control ZFEs.

Third, we determined the effect of MeHg exposure on movement by investigating both spontaneous movement and elicited movement as well as on NMJ development. We hypothesized that experimental groups will demonstrate less spontaneous and elicited movement. We determined effects of MeHg exposure on the NMJ by investigating AChRs and presynaptic vesicles. Since MeHg disrupts neuronal development and results in muscle abnormalities it was important to investigate components of the NMJ. We hypothesized that MeHg exposed ZFEs would show a quantitative decrease in clusters of AChRs and presynaptic vesicle aggregates when compared to controls.

II. MATERIALS AND METHODS

Animals

Adult wild-type zebrafish of the AB/TL strain were raised in the Department of Biology at Texas A&M University and kept under standard laboratory conditions at an ambient temperature of approximately 28.0ºC (Westerfield, 2000). Male and female adult zebrafish were placed in adjacent containers but separated by a barrier in the evening, and then paired at approximately 8 a.m. the following morning so eggs could be laid and fertilized. Fertilized embryos were obtained at approximately 10 a.m. in the morning. All ZFEs were held in an incubator with a constant temperature of 28.5ºC after transfer from the Biology Department. Embryo medium, consisting of ultrapure water containing low concentrations of specific ions and adjusted to pH 7.2, was used to maintain the developing ZFEs and was freshly prepared for each experiment according to Westerfield (2000). All ZFEs were staged and fixed at specific hours post fertilization (hpf) as described by Kimmel et al. (1995). Both adult and embryonic ZFEs were maintained according to protocols that were carried out in accordance with the National Institutes of Health Guide for the Care and Use of Laboratory Animals (National Institutes of Health Publication no. 85-23, revised 1996) and were approved the Texas A&M University Institutional Animal Use and Care oversight committee.

Methylmercury preparation and exposure

In this study we used three groups of ZFEs: controls (0 ppb MeHg), ZFEs exposed to 10 ppb MeHg and ZFEs exposed to 50 ppb MeHg. We prepared the different concentrations of MeHg in parts per billion (µg/L) in freshly prepared embryo medium. All MeHg stock solutions were stored at 4ºC until used. Embryo medium consisted of ultrapure water containing low concentrations of specific ions and adjusted to pH 7.2. The two experimental groups were exposed to MeHg for 24 hours using 24-well, flat-bottom plates with low evaporation lids (BD Biosciences, San Jose, CA, USA). In each experiment some ZFEs were placed in embryo medium without MeHg to serve as negative controls. The total volume of embryo medium in each well was 2ml. Two to three ZFEs were added to each well such that a minimum of 48 ZFEs were tested at each concentration of MeHg. After 24 hours of exposure ZFEs were placed in fresh embryo medium without MeHg for the duration of the study.

The covered 24-well plates were incubated for 72 hours at 28.5ºC (Thelco Laboratory Incubator; Cole-Palmer Instrument, Vernon Hills, IL, USA). 72 hours after fertilization the embryos were euthanized by chilling on ice and fixed in 10% neutral buffer formalin (NBF) for two hours at room temperature then stored at 4ºC in phosphate buffered saline (PBS) until used. Assessment of developmental and neurological abnormalities included measuring: mortality rate, hatching rate, overall length, yolk sac area, heart rate, heart volume, ventricle thickness, pericardial cavity volume, spontaneous movement, elicited movement, and quantification of acetylcholine receptors

and synaptic vesicles associated with neuromuscular junctions located on skeletal muscle. The experiment was repeated in triplicate.

Morphological assessment

The effects of exposure to different concentrations of methylmercury on ZFE morphology were assessed at multiple time points, using a SZ-40 binocular dissecting microscope (Olympus, Center Valley, PA, USA). ZFEs were examined at room temperature (25ºC) to monitor the developmental stage, mortality, hatching, spontaneous movement, response to touch, presence of deformities and heart rate.

Mortality and hatching rate

Mortality rate was determined by counting the number of dead ZFEs per group at 24 hpf, 48 hpf and 72 hpf. Dead embryos were removed at each monitoring time point. Hatching rate was determined by counting the number of hatched ZFEs per group at 48 hpf and 72 hpf. Hatched embryos were noted and kept in the wells until the end of the experiment.

Length and yolk sac

Ten fixed, hatched ZFEs from each group were placed in coded vials so the investigator was unaware of the treatment group being scored. Each ZFE was photographed and measured (See Figure 7). Each ZFE was placed in fresh PBS in a microscope well slide and viewed using a Nikon DS-Ri1 digital camera connected to a Nikon Eclipse E400 microscope to measure body length and yolk sac area.

ZFEs body length was taken from the tip of the head to the tip of the tail, excluding the median finfold. Yolk sac area was taken by outlining the entire yolk sac area. Two undergraduate students independently measured length and yolk sac area. If measurements of the two students differed by more than +/- 5%, that particular group was measured a third time by one of the original students. The student measurements were averaged for each ZFE used.

Both body length and yolk sac data demonstrated high variability so the controls were assessed first for any difference using a one-way ANOVA. There was a significant difference ($p = 0.011$) between the lengths of the three replicate control groups, so percent control was used to analyze body length. The computer software program, Image J (U.S. National Institutes of Health, Bethesda, MD, USA) was used to complete these measurements.

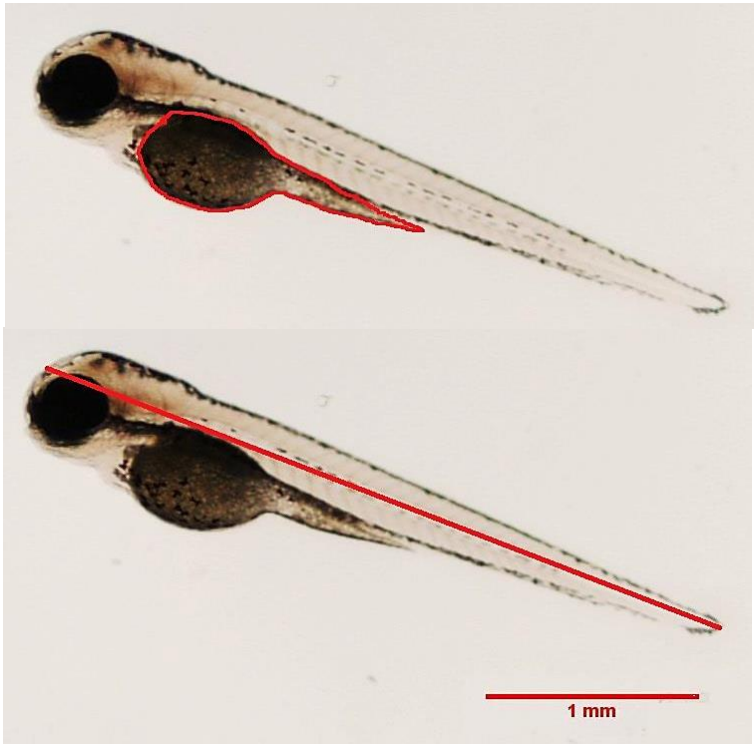

Figure 7. Yolk sac area and length measurements. Top picture demonstrates yolk sac area measurement; bottom picture demonstrates length measurement. Both measurements outlined in red.

Heart rate

At 72 hpf ZFEs were placed in a light anesthetic concentration of 0.3mM of MS-222 for 15 minutes, which immobilizes the embryo, but does not affect the heartbeat (Stehr et al., 2006). After the 15 minutes each ZFE was placed on its side in a petri dish filled with embryo medium and their heartbeats were counted for 10 seconds. Heartbeats were observed under the SZ-40 binocular dissection microscope with an N = 10 per group.

Sectioning and hematoxylin and eosin staining (H&E)

Fixed ZFEs were processed and embedded in paraffin, serially sectioned (5µm sagittal sections), mounted on plus-coated microscope slides and stained with Hematoxylin and Eosin (H&E).

Heart measurements

H&E stained sections were viewed using a Nikon DS-Ri1 digital camera connected to a Nikon Eclipse E400 microscope, and heart volume, ventricle thickness and pericardial cavity volume were measured using the NIS-Elements computer software program (Nikon Instruments Inc., Melville, NY, USA). Slides were coded to blind the investigators as to the treatment group during assessment. For pericardial and heart volume assessment we measured the area of the pericardial cavity and heart (See Figure 8) from each section and by including section thickness, calculated the volume of the heart and pericardial cavity. For ventricle thickness we measured the thickness of the ventricle (See Figure 9) from every third section taken through the ventricle of each embryo and then determined the averaged thickness of each ZFE. N = 7 was used for all measurements.

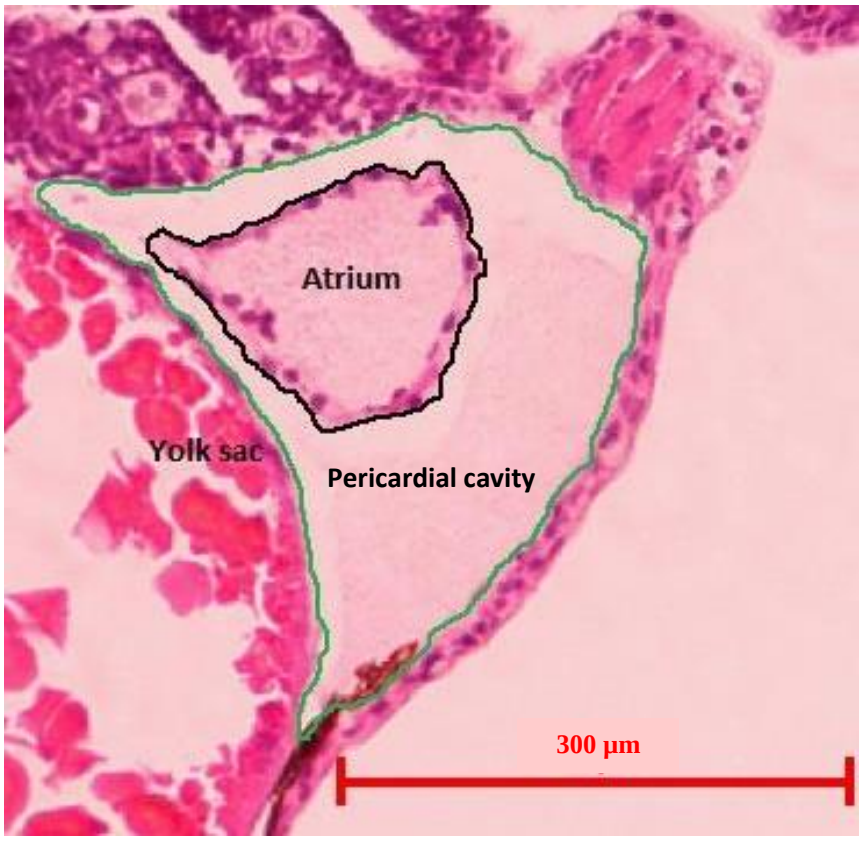

Figure 8. Heart and pericardial cavity measurements. Heart area measurement outlined in black. Pericardial cavity area measurement outlined in green.

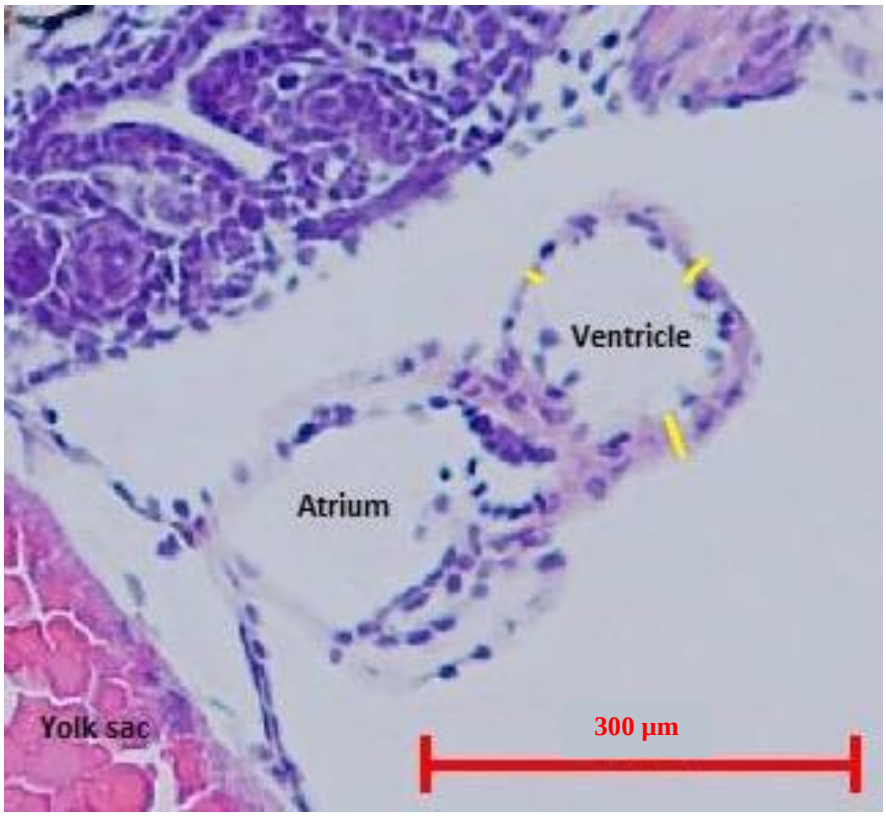

Figure 9. Ventricle thickness measurements. Measurement in yellow.

Spontaneous and elicited movement

Spontaneous movement was determined by observing the movement of all unhatched ZFEs per group, at approximately 30 hpf, using a SZ-40 binocular dissection microscope. The clear chorion allowed total visibility to observe spontaneous movements during one minute of observation. Spontaneous movement is an indicator of primary motor neuron innervation of the skeletal muscle and can be observed as a twitch

or slight movement of the ZFE tail. For elicited movement 10 hatched ZFEs were assessed per group. At 72 hpf each ZFE was individually placed in a petri dish containing fresh embryo medium with a grid underneath the transparent dish. The grid consisted of squares that were each 5mm on a side. Elicited movement was conducted by touching the tail of each ZFE up to 4 times with the tip of an insect pin, while observing through the SZ-40 binocular dissection microscope. The distance traveled was calculated by counting the number of squares the embryo traveled and multiplying by 5mm.

Immunohistochemistry and AChR staining

Whole fixed ZFEs were permeabilized for 30 minutes in 4% Triton-X 100 containing 2% bovine serum albumin (BSA) and 10% goat serum then incubated for 48 hours at 4ºC in mouse monoclonal SV2 (1:100; Developmental Studies Hybridoma Bank, University of Iowa, Iowa City, IA, USA), which targets the synaptic vesicle protein, SV2, on pre-synaptic vesicles. ZFEs were washed in PBS for 2-3 hours and then incubated for 4 hours at room temperature in secondary antibody, goat anti-mouse IgG coupled to Cy3 (1:2000; Jackson ImmunoResearch, West Grove, PA, USA). ZFEs were washed in PBS for 2 hours then mounted in glycerol for viewing. To insure specific staining, controls were utilized: (1) ZFE with no staining, (2) ZFE stained with SV2 only and no secondary antibody, (3) ZFE stained with secondary antibody coupled with Cy3 and no primary antibody. Another set of ZFEs were incubated in Alexa Fluor 488-conjugated α-bungarotoxin (1μM; Molecular Probes (Life Technologies) Grand Island,

NY, USA) for 30 minutes after permeabilization to label ACh receptors. ZFEs were washed in PBS for 2 hours and mounted in glycerol for viewing. To insure specific staining, controls were utilized that consisted of observing ZFE with no staining. All embryos were imaged on a Zeiss 510 Meta confocal microscope and photographed under a 40X objective. Images were compiled using Zeiss 510 Meta confocal image browser software as z-stack compilations of half the trunk.

Immunohistochemistry assessment

Images taken of IHC stained ZFEs were converted to tif images and we used NIS-elements to count stained AChR associated with primary motor neuron axons extending between skeletal muscle bundles (See Figure 10). AChR clusters were counted between skeletal muscle bundles 10 and 11 and between muscle bundles 11 and 12. Two lengths of about 38 μm were measured and AChR clusters were counted within these lengths. NIS-elements was used to count aggregates of presynaptic vesicles. Two areas of 625μm^2 were blindly measured and aggregates of presynaptic vesicles were counted within these areas for each ZFE (See Figure 11). ZFEs image were coded to blind the investigator as to which groups were being assessed.

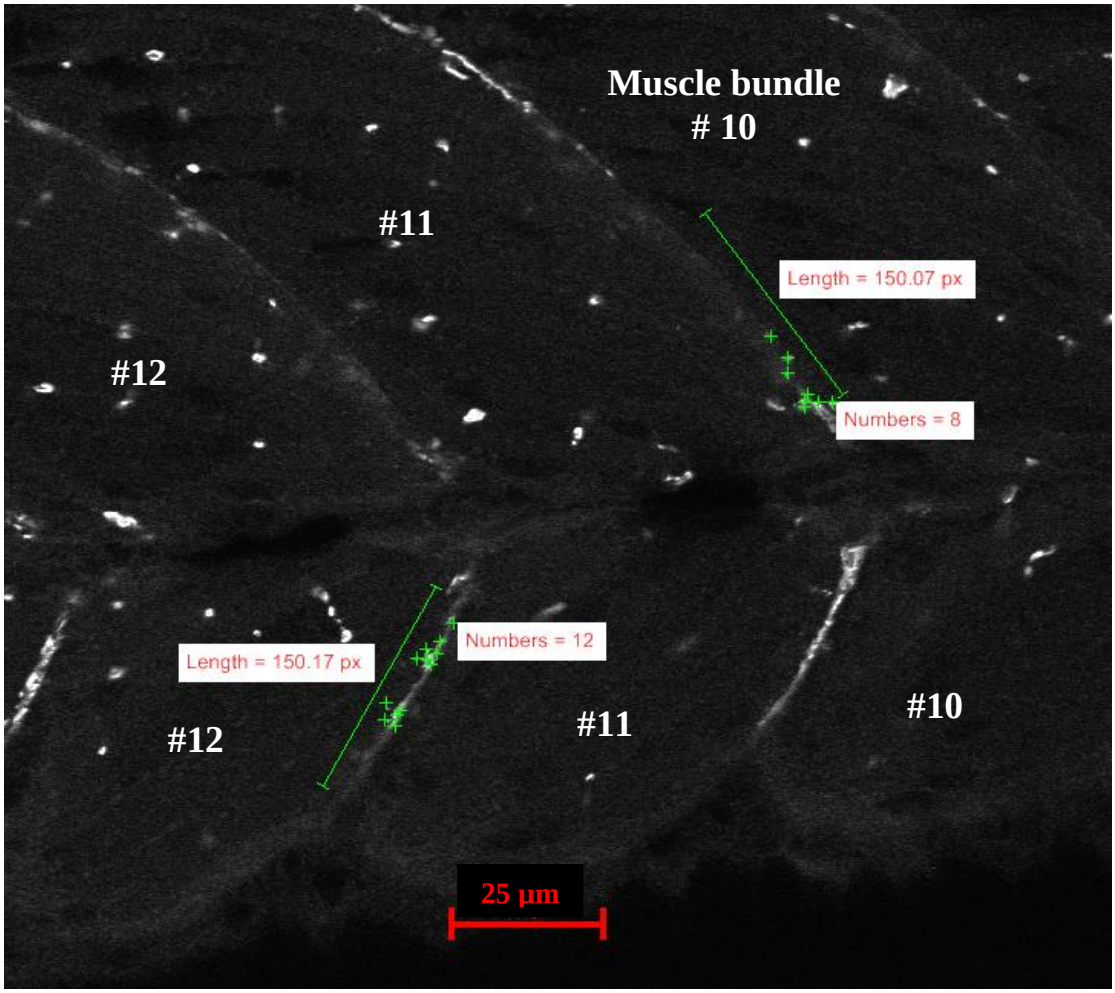

Figure 10. AChR cluster counting. Each length was about 150 pixels = 37.5 µm. Numbers counter refers to AChR cluster count.

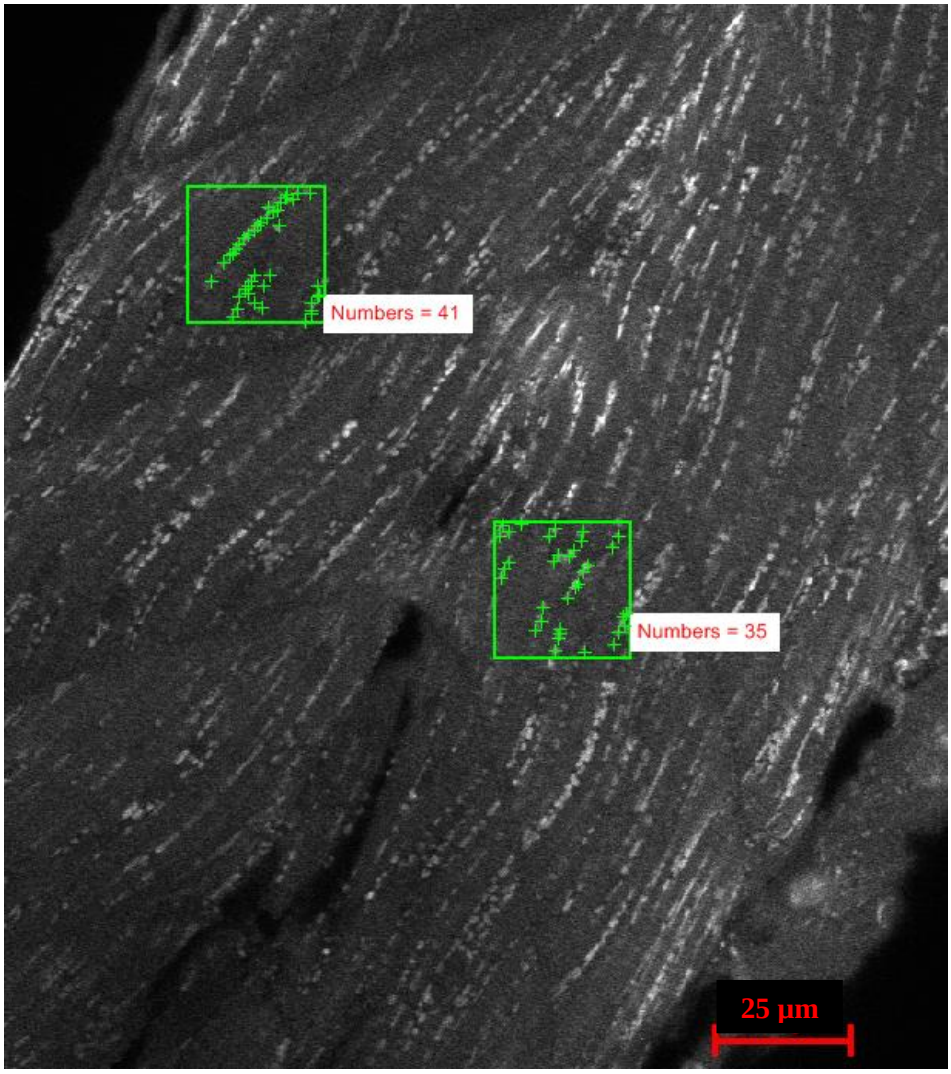

Figure 11. Presynaptic vesicle aggregate count. Each box is 625 µm^2. Number counter refers to the number of presynaptic vesicle aggregates counted in that area.

Statistical analysis

All data were analyzed using SPSS 12.0 for Windows and one-way ANOVAs were run. Significance was set at $P \leq 0.05$. If there was a significant difference demonstrated then Tukey's HSD post hoc test was used. Chi square was used to analyze elicited movement and spontaneous movement.

III. RESULTS

General developmental affects

Mortality rate

Morality rate was calculated for each group per set, and the averages were compared across all three sets, yielding a sample size of 3 per group. These data were analyzed using a one-way ANOVA. No significant difference in mortality rate was determined ($p = 0.988$; See Figure 12). These data demonstrate that neither MeHg concentration used in this study caused increased ZFE death compared to control ZFEs. This particular study was focused on understanding neurotoxic mechanisms underlying nonlethal MeHg exposure on the developing nervous system, so the observed low mortality rate was expected and appropriate for this study.

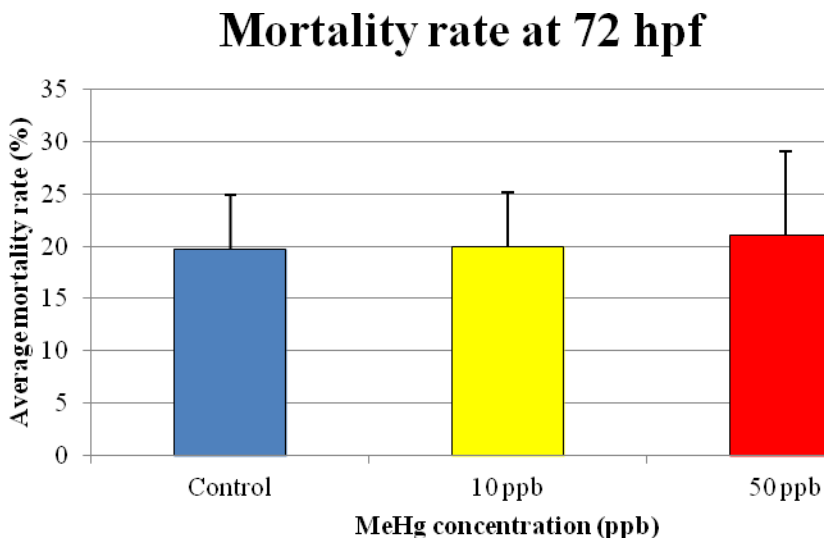

Figure 12. Mortality rate at 72 hpf. Mortality rate was observed at 24 hpf, 48 hpf and 72 hpf. N = 3 across all groups. No significant difference was observed (p = 0.988).

Hatching rate

The hatching rate was calculated as percentage of total live ZFEs for each group per set, with three sets in each group, and these percentages were averaged across all sets. These data were analyzed using a one-way ANOVA. No significant difference was observed (p = 0.628; See Figure 13). MeHg exposure has been shown to delay or inhibit ZFEs ability to hatch from the chorion. Therefore, ZFEs were expected to hatch later resulting in lower hatching rates. A study conducted by Hassan et al. (2012) demonstrated that 92% of control ZFEs hatched by 72 hpf while this study demonstrated an average of 43% hatched rate by 72 hpf. ZFEs exposed to 10 ppb MeHg demonstrated

an average of 47% hatched rate and ZFEs exposed to 50 ppb MeHg demonstrated an average of 54% hatched rate.

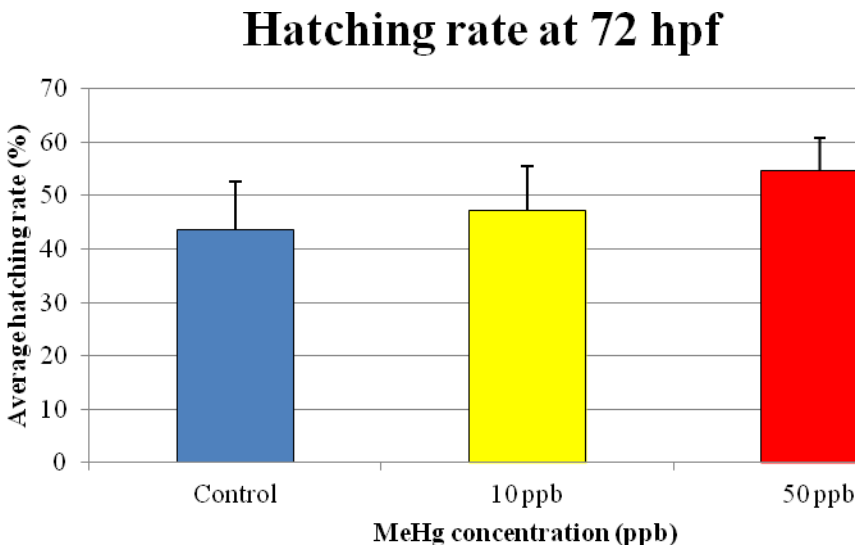

Figure 13. Hatching rate at 72 hpf. Hatching rate was observed at 48 hpf and 72 hpf. N = 168 across all groups. No significant difference (p = 0.628).

Length

Percent control was used to analyze these data due to a significant difference (p = 0.011) observed among the three replicate control groups. These data were analyzed using one-way ANOVA. A statistical difference was determined between 50 ppb and the other two groups (p = 0.0001; See Figure 14). These data suggest that exposure at 50 ppb MeHg decreased the length of ZFEs. MeHg exposure has been associated with delayed development, which could account for the shorter lengths of ZFEs exposed to 50

ppb MeHg. Since an increase in length correlates with a decrease in yolk sac area, a decrease in length should correlate with in an increase in yolk sac area.

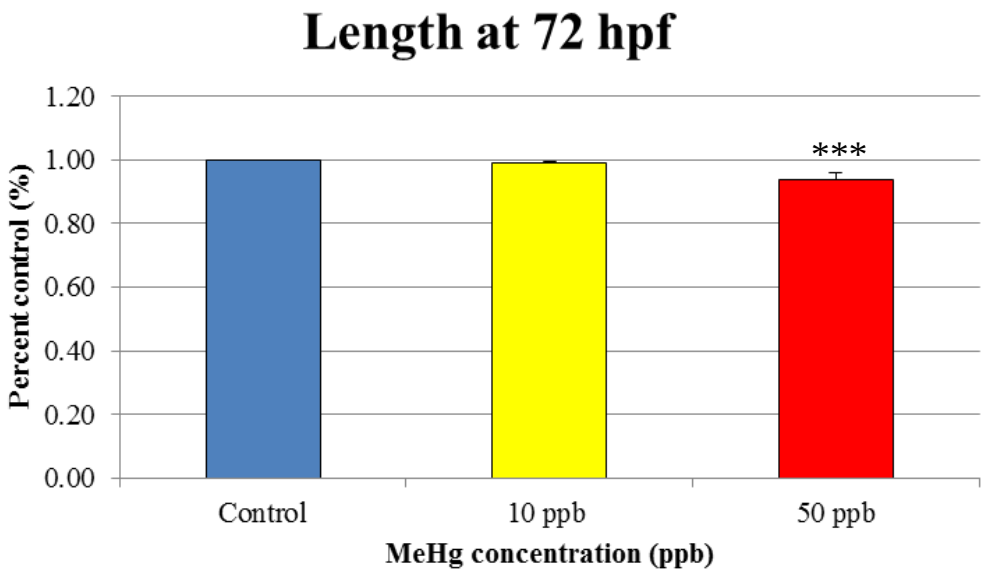

Figure 14. Length at 72 hpf. N = 26 for controls and 10 ppb, and N = 27 for 50 ppb. A significant difference (p = 0.0001) between 50 ppb and control and 10 ppb was determined, using Tukey's HSD test. p < 0.001 = *.**

Yolk sac area

No significant difference was observed (p = 0.425) among the three replicate control groups so the averages from each set per group was combined and analyzed with a one-way ANOVA (See Figure 15). No significant difference in yolk sac area was observed (p = 0.115). However, a trend towards increased yolk sac area was observed in ZFEs treated with 50 ppb MeHg. MeHg exposure has been associated with delayed

development which could result in shorter length of the embryos, which correlates with increased yolk sac area. Since MeHg exposure demonstrated developmental delays other aspects of ZFE development was investigated such as heart development.

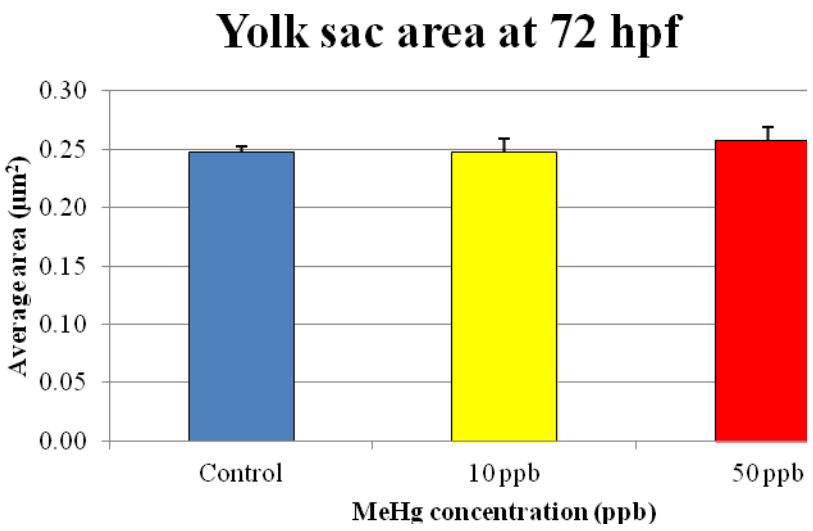

Figure 15. Yolk sac area at 72 hpf. N = 26 for controls and 10 ppb, N = 27 for 50 ppb.

Heart developmental affects

Heart rate

Percent control was calculated and analyzed using one-way ANOVA (See Figure 16). A statistical difference was determined ($p = 0.026$). The Tukey's HSD post hoc test was used to determine differences between groups where the controls differed from ZFEs exposed to 50 ppb MeHg ($p = 0.043$), but not between control ZFEs and ZFEs exposed to 10 ppb MeHg ($p = 0.994$). These data suggest that MeHg exposure at 50 ppb significantly decreased heart rate. MeHg exposure in humans has demonstrated an adverse effect on the cardiovascular system resulting in various heart diseases. Thus, abnormal cardiovascular function could contribute to the observed decrease in heart rate. Since MeHg exposure has an effect on heart rate other heart parameters were also investigated.

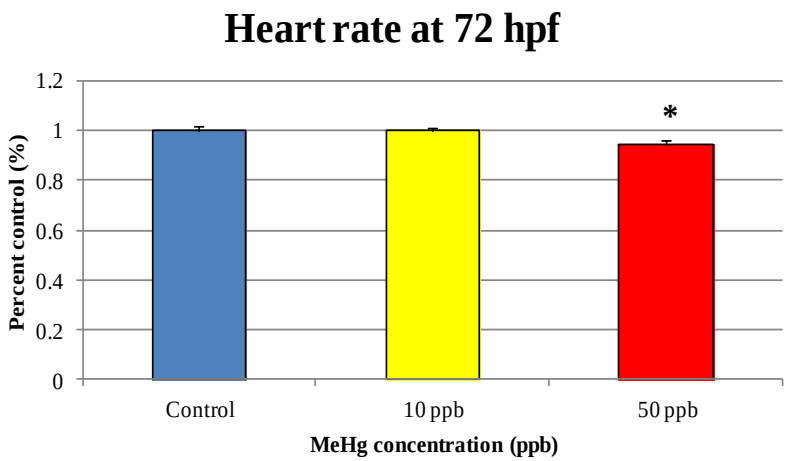

Figure 16. Heart rate at 72 hpf. N = 30 across all groups. A significant difference between controls and 50 ppb (p = 0.043) was determined, using Tukey's HSD test. p < 0.05 = *.

Heart volume

The volume of the heart was analyzed using one-way ANOVA (See Figure 17). No significant difference was demonstrated (p = 0.641), indicating that MeHg exposure had no effect on heart volume. Although, MeHg exposure did not affect heart volume further investigation of the heart was conducted by assessing ventricle thickness.

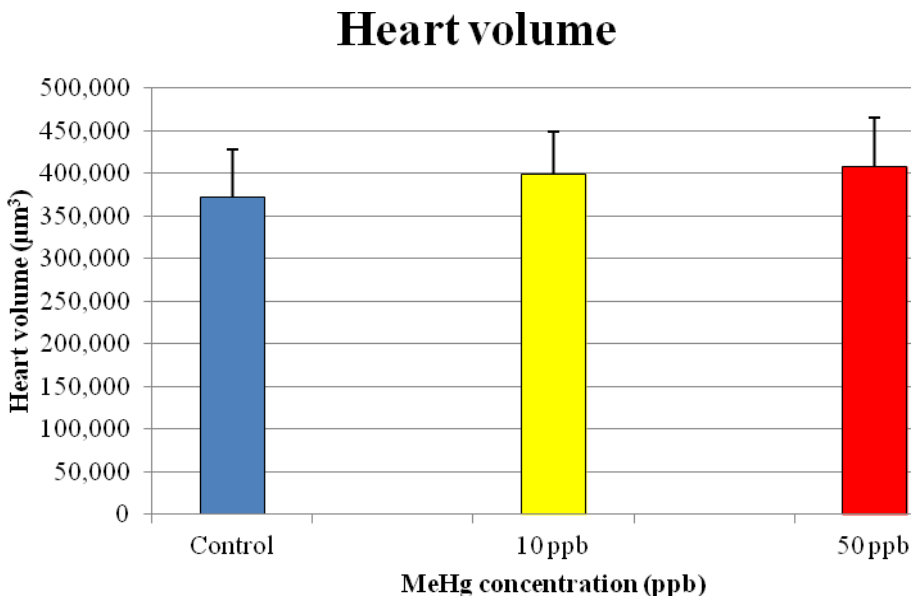

Figure 17. Heart volume. N = 7 across all groups.

Ventricle thickness

An average of three ventricle thickness measurements for seven ZFEs in each group were calculated and analyzed with one-way ANOVA (See Figure 18). No significant difference was demonstrated ($p = 0.421$). This indicates that MeHg exposure did not have an effect on ventricle thickness. MeHg exposure has been reported to affect the cardiovascular system, though it does not seem to affect morphology of the heart with respect to heart volume and ventricle thickness.

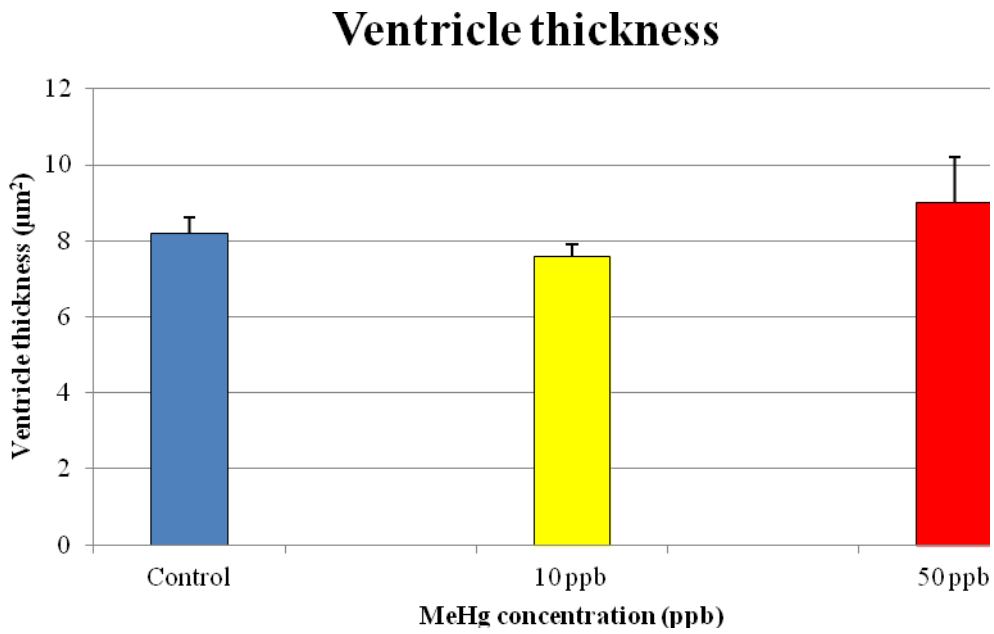

Figure 18. Ventricle thickness. N = 7 across all groups.

Pericardial cavity volume

The volume of the pericardial cavity was calculated and analyzed with one-way ANOVA (See Figure 19). No significant difference was demonstrated ($p = 0.090$), though a trend towards increased pericardial cavity volume was observed in ZFEs exposed to 50 ppb MeHg. MeHg exposure has been associated with edema of the pericardial cavity in hamsters. A trend towards increasing pericardial cavity volume could be associated with impaired cardiovascular system of ZFEs exposed to 50 ppb MeHg. MeHg exposure did not result in morphological abnormalities of cardiac muscle as far as heart volume and ventricle thickness is concerned. But MeHg exposure could

have affected skeletal muscle where investigation of movement was assessed.

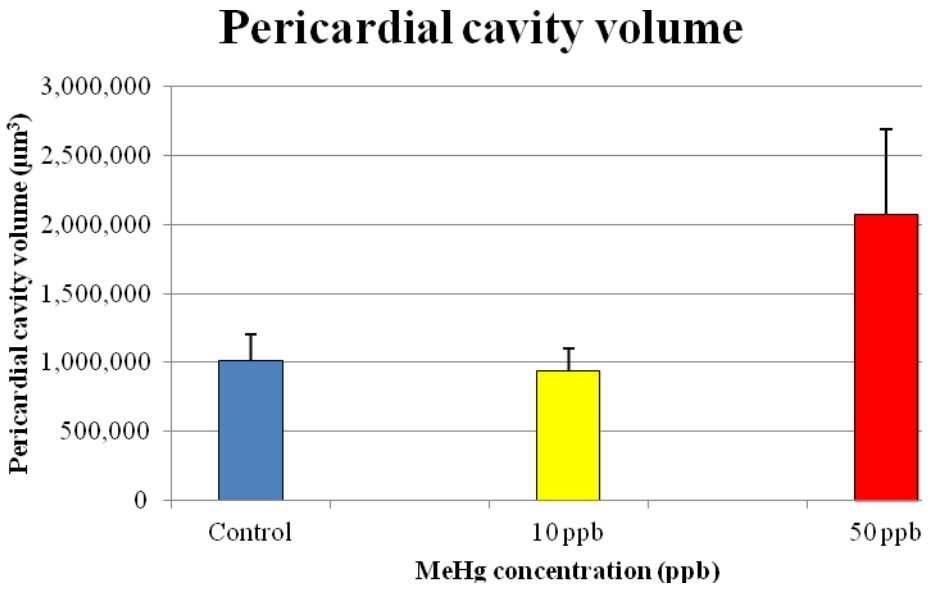

Figure 19. Pericardial cavity volume. N = 7 across all groups.

Spontaneous and elicited movement

Spontaneous movement

Percent control was used to normalize the data so the three experimental replicates could be combined for analysis. The percentage of ZFEs that exhibited any amount of spontaneous movement was analyzed using a one-way ANOVA and a statistical difference was observed ($p = 0.004$). The Tukey's HSD post hoc test was used

to determine that control ZFEs differed from ZFEs exposed to 10 ppb MeHg ($p = 0.004$) as well as ZFEs exposed to 50 ppb MeHg ($p = 0.020$; See Figure 20). These data suggest that MeHg exposure significantly decreased the number of ZFEs that exhibited spontaneous movement.

Next, for the subset of ZFEs that exhibited spontaneous movement we assessed how many times each ZFE moved during the assessment time of one minute. The percent of spontaneous movements in each category (1 to 7 movements per minute) was calculated for each experimental group (See Table 2). These data were analyzed using Chi-square with 12 degrees of freedom and we determined that control ZFEs were significantly different from ZFEs exposed to 10 ppb MeHg ($p = 0.0001$). Chi-square analysis also demonstrated a significant difference between control ZFEs and ZFEs exposed to 50 ppb MeHg ($p = 0.0001$). These data indicate that MeHg exposure significantly decreased the number of spontaneous locomotor movements demonstrated per ZFE.

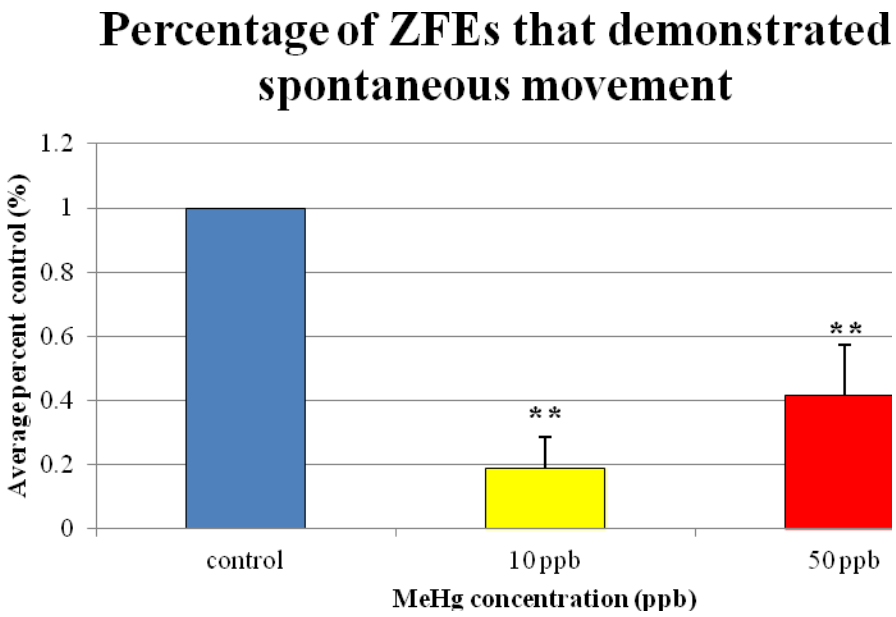

Figure 20. Percentage of ZFEs that demonstrated spontaneous movement. Spontaneous movement observed at 24 hpf. N = 3 across all groups. A significant difference between controls and 10 ppb ($p = 0.004$) and 50 ppb ($p = 0.020$) was determined, using Tukey's HSD test. $p < 0.05$ = *, $p < 0.01$ = **.

Table 2. Percent of ZFE that demonstrated 1 to 7 spontaneous movements.

# of movements	Control	10 ppb	50 ppb
1	**48**	**83**	**63**
2	**17**	**8**	**13**
3	**9**	**0**	**23**
4	**14**	**0**	**0**
5	**4**	**2**	**0**
6	**1**	**8**	**0**
7	**8**	**0**	**0**

Elicited movement

The distance traveled by each embryo was calculated, and categorized into 5 categories. These data were analyzed using Chi-square (See Table 3) with 4 degrees of freedom, which demonstrated no significant difference between control ZFEs and ZFEs exposed to 10 ppb MeHg ($p = 0.421$). There was a significant difference between control ZFEs and ZFEs exposed to 50 ppb MeHg ($p = 0.001$) as well as between ZFEs exposed to 10 ppb MeHg compared to ZFEs exposed to 50 ppb MeHg ($p = 0.008$). These data indicate that ZFEs exposed to 50 ppb MeHg swam significantly less distance when touched to induce elicited movement.

Table 3. Number of ZFEs that moved in each distance category.

Movement (mm)	Control	10 ppb	50 ppb
0	**1**	**4**	**14**
1 - 5	**6**	**3**	**7**
6 - 10	**7**	**4**	**1**
11 - 15	**1**	**1**	**1**
16 +	**15**	**18**	**7**

Neuromuscular junction development

Acetylcholine receptors

AChR clusters were counted per unit length between two adjacent muscle bundles in the trunk. The average numbers of AChR cluster per unit length for each ZFE were calculated and analyzed using one-way ANOVA (See Figure 21). No significant difference ($p = 0.305$) was observed across all groups. Though, a trend toward decreasing number of AChR clusters was observed in ZFEs exposed to MeHg. A significant difference may have been masked due to high variability among the groups. ZFEs exposed to MeHg demonstrate skeletal muscle abnormalities, which could be why we see a trend towards a decrease in the number of AChR clusters observed at the NMJ.

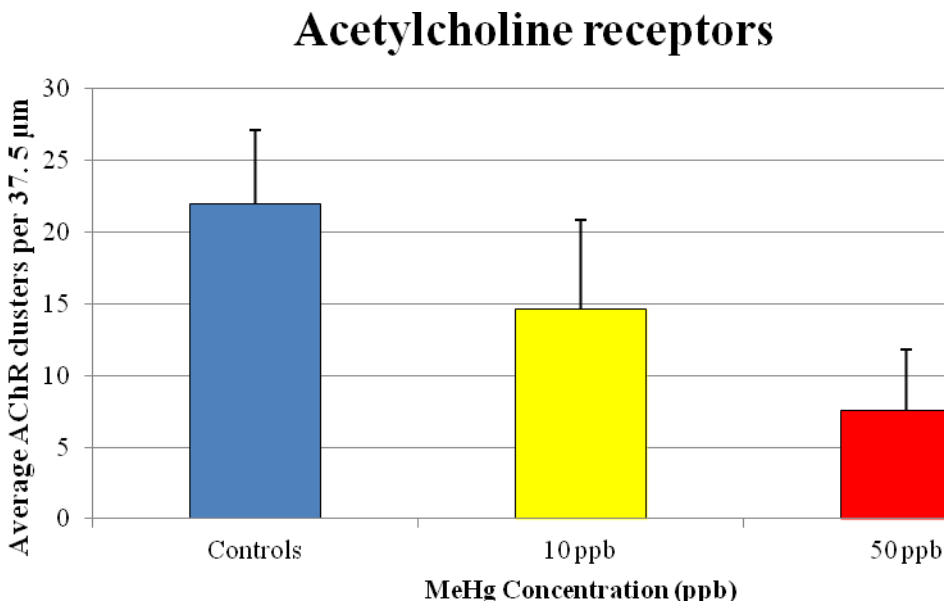

Figure 21. Acetylcholine receptors. N = 5 across all groups.

Presynaptic vesicles

Presynaptic vesicle aggregates were counted per unit area. The average numbers of presynaptic vesicle aggregates were calculated and analyzed using one-way ANOVA (See Figure 22). No significant difference was observed ($p = 0.434$). These data suggest that MeHg exposure has no effect on presynaptic vesicles density.

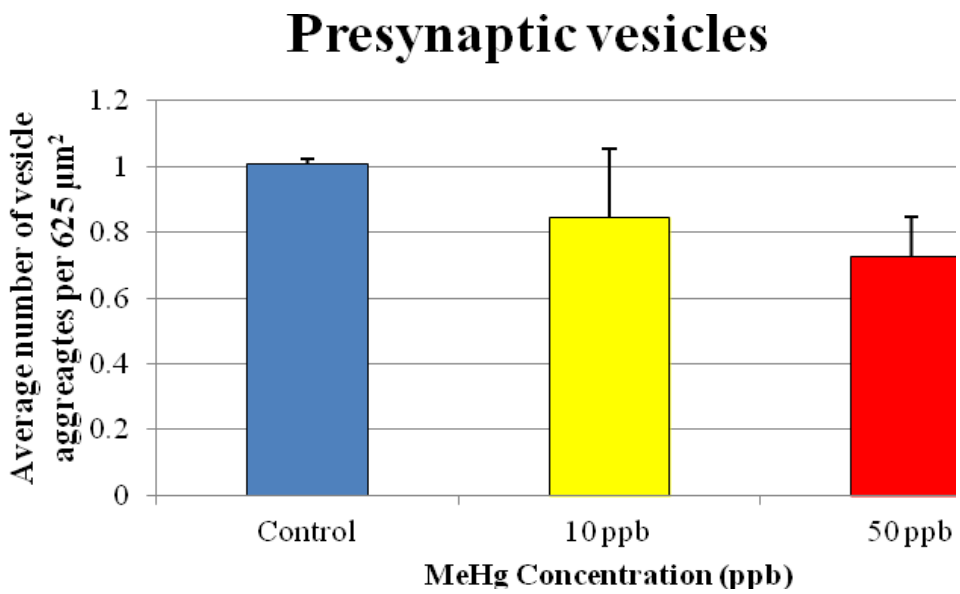

Figure 22. Presynaptic vesicles. N = 3 across all groups.

IV. DISCUSSION

General developmental effects

The purpose of this study is to better understand the neurotoxic mechanisms of MeHg on the developing nervous system. To understand the effects of MeHg on the nervous system we first, investigated the effects of MeHg on general ZFE development. Previous studies have looked at developmental effects of MeHg exposure in ZFEs and have determined that high concentrations of MeHg result in developmental delays, high mortality rates, and delay or inhibition of ZFEs ability to hatch. However, in this study we used very low concentrations of MeHg exposure (10 and 50 ppb), which are in the range of current human exposure to MeHg (Myers et al., 2003)

Mortality and hatching rate

We did not observe any increase in mortality with the concentrations of MeHg used in this study. This is in agreement with a previous study by Hassan et al. (2012). Because this study focused on understanding neurotoxic mechanisms underlying nonlethal MeHg exposure on the developing nervous system, the observed low mortality was expected and appropriate for this study. Based on these observations, it is possible that a somewhat higher concentration of MeHg could be used in future experiments.

However, exposure to MeHg at concentrations above 80 ppb have been reported to result in significant ZFE mortality (Hassan et al., 2012).

No difference in hatching rate was observed in this study. This is different from what was observed by Hassan et al. 2012. In the Hassan (2012) study about 92% of control ZFEs hatched by 72 hpf and ZFEs exposed to 20 and 50 ppb exhibited significantly less hatching at 72 hpf. In this study control ZFEs demonstrated an average 43% hatched rate by 72 hpf. One possible explanation for this difference was that the ZFEs used in this study were from different zebrafish stocks than the ZFEs used in the Hassan et al., 2012 study. Different baseline development rates could exist and a slower baseline hatching rate may have masked subtle differences in hatching rates produced by exposure to MeHg.

Length and yolk sac area

ZFEs contain a yolk sac, which serves as the sole source of nutrition during early development. Throughout the developmental process the yolk sac decreases in area, which correlates with growth of the ZFE as seen by increasing ZFE length. MeHg exposure has been known to cause delayed development. Delayed development could explain the presence of a larger than normal yolk sac. In this study MeHg exposure decreased body length of ZFEs exposed to 50 ppb MeHg. Since an increase in length correlates with a decrease in yolk sac area a decrease in length should correlate with an increase in yolk sac area.

Yolk sac area showed no significant difference but there was a trend towards increased yolk sac area in ZFEs exposed to 50 ppb MeHg. This trend is consistent with the decreased body length in this same group of ZFEs, suggesting that MeHg exposure delays development. These data could also reinforce the possibility that the ZF stock used in this study may have a difference baseline development rate that could have been compounded with MeHg exposure.

A delay in development due to MeHg exposure also could be reflected in development of various organs. Many processes must be completed before a ZFE hatches, and if MeHg exposure delays these processes then the ZFE could develop health problems due to under developed organs. We investigated the effects of MeHg exposure on heart development.

Heart effects

Several studies have shown that MeHg exposure can lead to coronary artery and carotid atherosclerosis, increased blood pressure, and myocardial infarction in humans (Guallar et al., 2002, Choi et al., 2008). An increase in heart rate has been associated with progression of coronary atherosclerosis (Tardif, 2009). Based on this information we initially believed that heart rate would increase in ZFEs exposed to MeHg, but we observed a significant decrease in heart rate of ZFEs exposed to 50 ppb MeHg compared to control ZFEs.

A study conducted on isolated heart preparations from guinea pigs demonstrated that due to the lipophilic nature of MeHg it was able to bind to thiol groups within the membrane of cardiac cells resulting in negative inotropic effect in heart tissues (Halbach, 1990). A negative inotropic effect in heart tissues results in less forceful contractions, which decreases heart rate. Thus, based on this study in guinea pig heart preparations MeHg exposure affected cardiac muscle cells in a manner that could decrease heart rate, which is consistent with our results.

We did not investigate specific mechanisms by which MeHg affected cardiomyocytes but we speculate that increased production of ROS could be a possible mechanism. It has also been reported that MeHg changes mitochondrial function in the developing rate brain (Bellum et al., 2007). This can disrupt the electron transport chain resulting in an increase in ROS byproducts within cells, including cardiac muscle. In support of this idea, several studies have reported that ROS and oxidative stress as important features of cardiovascular diseases including atherosclerosis, hypertension and congestive heart failure (Sugamura and Keaney Jr, 2011).

Since MeHg exposure decreased the heart rate of ZFEs, we investigated other parameters of ZFE heart development including heart volume, ventricle thickness and pericardial volume. It has been demonstrated that MeHg exposure could lead to heart disease in humans and edema of the pericardial cavity in hamsters (Gale, 1981, Guallar et al., 2002, Choi et al., 2008). Therefore, by investigating these parameters we will better understand the effect of MeHg exposure on heart development. Heart volume and ventricle thickness data suggest that MeHg exposure does not affect heart morphology

but a trend towards an increase in pericardial cavity volume was observed. The space between the visceral pericardium and parietal pericardium is called the pericardial cavity, which contains serous fluid to allow the heart to contract/move within the body cavity without encountering friction. Edema of the pericardial cavity or pericardial effusion occurs when too much serous fluid is produced. Edema can result from inflammation of the pericardium, myocardial infarction as well as an impaired cardiovascular system. The trend observed towards an increase in pericardial cavity volume as well as a decrease in heart rate both suggest impaired cardiovascular system.

These data suggest that future experiments should examine heart function and morphology, including assessment of the pericardial cavity in older ZFEs and even in adult zebrafish that have been exposed to low concentrations of MeHg. It is possible that the adverse effects observed at 72 hpf could get progressively worse as the ZFEs mature.

Movement effects

MeHg exposure has resulted in the destruction and/or demyelination of the dorsal root of spinal nerves as well as damage to the cerebral cortex and cerebellum. These detrimental effects of MeHg exposure will result in abnormal movement so we examined spontaneous and elicited movement in ZFEs exposed to MeHg. Spontaneous locomotor movement is typically displayed in developing ZFEs and indicates that initial neuronal innervation from primary motor neurons is occurring in skeletal muscle of the trunk and tail. In this study MeHg exposure decreased the percentage of ZFEs that

demonstrated spontaneous movement as well as the number of movements demonstrated by each ZFE. These data suggest that MeHg exposure could either prevent innervation of the muscle by primary motor neurons or it could reduce the amount of spontaneous movement through prevention of muscle contractions. Another possibility is that since MeHg exposure can delay development, perhaps the stage of development at which spontaneous movement was assessed in ZFEs exposed to MeHg was effectively earlier than the developmental age of the control ZFEs and the MeHg exposed ZFEs exhibited less spontaneous movement.

We observed an adverse effect of MeHg on spontaneous movement in ZFEs at 30 hpf, and observed ZFE movements later in development could provide further insight of MeHg exposure on developing skeletal muscle. Therefore, elicited movement was another parameter that we investigated. We observed that MeHg exposure decreased elicited movement in ZFEs exposed to 50 ppb MeHg. ZFEs exposed to MeHg often displayed kinked tails, which could have hindered their ability to swim properly. So instead of these ZFEs swimming a straight trajectory some swam in a circle, displayed uncoordinated swimming movements or did not swim at all.

Sensory neurons send impulses to the CNS where it is processed by the cerebellum in order to coordinate the proper motor action. Motor fibers then send an impulse to skeletal muscle where a specific action will then take place. Perhaps sensory neurons were not able to send information to the CNS, preventing the action of swimming away from occurring. Or the sensory neurons were able to send an impulse to the CNS but due to damage of the cerebellar granule cells a coordinated swimming

action could not be integrated into a fine-tuned motor action. It would be interesting to examine the cerebellum of 73 hpf ZFEs to see if they have fewer granule cells present, since these specific neurons are highly susceptible to MeHg toxicity.

Neuromuscular junction effects

ZFEs exposed to MeHg demonstrated muscle abnormalities, which could be due to abnormalities at the neuromuscular junction or abnormalities that are intrinsic to muscle structure or both. The neuromuscular junction has many essential components but the ones we assessed were acetylcholine receptors (AChRs) and presynaptic vesicles. One important thing to note is that both AChRs and presynaptic vesicles cannot be individually counted at the light microscope level due to their extremely small size, but AChR clusters and aggregates of synaptic vesicles can be counted using a light microscope. We observed a trend towards decreasing numbers of AChR clusters in experimental ZFEs. Because we are counting clusters of AChRs the actual number of AChRs could be significantly decreased in experimental groups. Presynaptic vesicles aggregates demonstrated no significant difference when exposed to MeHg.

MeHg exposure has been known cause an increase in ROS, which could result in neuronal apoptotic death. A study using cultured cerebellar granule neurons demonstrated that ROS formation can lead to necrosis and apoptosis of these neurons (Valencia and Morán, 2004). One possible explanation for the trend of decreasing numbers of AChR clusters in experimental ZFEs could be that MeHg exposure produced

neuronal cell death that could result in loss of and/or redistributing AChR clusters on skeletal muscle. Since the AChR clusters were counted and not the actual number of AChRs perhaps MeHg exposure has more of an impact on AChRs than these data are demonstrating.

One important issue that was noted is that the presynaptic vesicle aggregates were observed at the NMJ of axons that branched off the primary motor neuron. While the AChR clusters were observed at the NMJ of the primary motor neurons. This means that the presynaptic vesicle aggregates that were assessed did not directly correlate with the AChR clusters that were assessed. However, both are components of the NMJs that are located on skeletal muscle cells, so it was reasonable to assess both parameters. It is not clear why the IHC staining for presynaptic vesicle aggregates did not clearly visualize the aggregates associated with NMJ innervated by primary neurons.

V. CONCLUSIONS

In this study MeHg exposure had adverse effects on ZFE development, specifically body length and possibly yolk sac area. Developmental delays can affect multiple body systems resulting in impaired function of these systems. Since heart volume and ventricle thickness demonstrated no significant difference across all groups at 72 hpf. But the observed trend towards increased pericardial cavity volume and the significant decrease in heart rate of ZFEs exposed to 50 ppb MeHg suggest MeHg exposure impaired cardiovascular system function. Thus, MeHg might adversely affect heart function without producing obvious morphologic defects. MeHg exposure can also lead to an increase in ROS and oxidative stress, which has been identified as important features of cardiovascular disease. We speculate that excessive generation of ROS might be a cause for defective cardiovascular function in the ZFEs. The changes observed in this study were subtle. It would be interesting to examine older ZFEs or even adult ZFEs to see if these changes are magnified as they age.

Spontaneous ZFE movement occurs during early development and indicates primary motor neuron innervation of skeletal muscle. MeHg exposure decreased spontaneous movement at 30 hpf and elicited movement was decreased at 72 hpf, which lead us to examine components of the NMJ. The trend towards decreased AChR clusters and no change in presynaptic vesicle aggregation suggest that MeHg exposure from 5 to 30 hpf has minimal effect on NMJ development at 72 hpf. It is possible that MeHg exposure from 5 to 30 hpf may have been more pronounced at 30 hpf but the

ZFEs recovered by 72 hpf. Another explanation is that MeHg has minimal effect on NMJ development and expression but directly affects skeletal muscle development and/or structure. Further investigation into skeletal muscle morphology and function are warranted.

The overall conclusion of this study is that exposure to 24 hours of low concentrations of MeHg, that cause slight delays in progression of development but no increased mortality, do not cause major cardiac muscle development or skeletal muscle innervation. It is likely that exposure to low MeHg concentrations result in functional deficits that are not reflected in obvious morphologic deficits.

REFERENCES

Allen JW, Mutkus LA, Aschner M (2001) Methylmercury-mediated inhibition of ^{3}Hd-aspartate transport in cultured astrocytes is reversed by the antioxidant catalase. Brain Research 902:92-100.

Aschner M, Yao CP, Allen JW, Tan KH (2000) Methylmercury alters glutamate transport in astrocytes. Neurochemistry International 37:199-206.

Bassett DI, Currie PD (2003) The zebrafish as a model for muscular dystrophy and congenital myopathy. Human Molecular Genetics 12:R265-R270.

Bellum S, Bawa B, Thuett KA, Stoica G, Abbott LC (2007) Changes in biochemical processes in cerebellar granule cells of mice exposed to methylmercury. International Journal of Toxicology 26:261-269.

Blader P, Strähle U (2000) Zebrafish developmental genetics and central nervous system development. Human Molecular Genetics 9:945-951.

Carvalho L, Heisenberg C-P (2010) The yolk syncytial layer in early zebrafish development. Trends in Cell Biology 20:586-592.

Chen WJ, Bōdy RL, Mottet NK (1979) Some effects of continuous low-dose congenital exposure to methylmercury on organ growth in the rat fetus. Teratology 20:31-36.

Choi AL, Weihe P, Budtz-Jørgensen E, Jørgensen PJ, Salonen JT, Tuomainen T-P, Murata K, Nielsen HP, Petersen MS, Askham J (2008) Methylmercury exposure and adverse cardiovascular effects in Faroese whaling men. Environmental Health Perspectives 117:367-372.

Davidson PW, Myers GJ, Cox C, Axtell C, Shamlaye C, Sloane-Reeves J, Cernichiari E, Needham L, Choi A, Wang Y (1998) Effects of prenatal and postnatal methylmercury exposure from fish consumption on neurodevelopment: outcomes at 66 months of age in the Seychelles child development study. JAMA 280:701-707.

Davidson PW, Myers GJ, Weiss B (2004) Mercury exposure and child development outcomes. Pediatrics 113:1023-1029.

Devoto SH, Melançon E, Eisen JS, Westerfield M (1996) Identification of separate slow and fast muscle precursor cells in vivo, prior to somite formation. Development 122:3371-3380.

Drapeau P, Saint-Amant L, Buss RR, Chong M, McDearmid JR, Brustein E (2002) Development of the locomotor network in zebrafish. Progress in Neurobiology 68:85-111.

Ekino S, Susa M, Ninomiya T, Imamura K, Kitamura T (2007) Minamata disease revisited: an update on the acute and chronic manifestations of methyl mercury poisoning. Journal of the Neurological Sciences 262:131-144.

Farina M, Rocha JB, Aschner M (2011) Mechanisms of methylmercury-induced neurotoxicity: evidence from experimental studies. Life Sciences 89:555-563.

Gale TF (1981) The embryotoxic response produced by inorganic mercury in different strains of hamsters. Environmental Research 24:152-161.

Guallar E, Sanz-Gallardo MI, Veer Pvt, Bode P, Aro A, Gómez-Aracena J, Kark JD, Riemersma RA, Martin-Moreno JM, Kok FJ (2002) Mercury, fish oils, and the risk of myocardial infarction. New England Journal of Medicine 347:1747-1754.

Halbach S (1990) Mercury compounds: lipophilicity and toxic effects on isolated myocardial tissue. Archives of Toxicology 64:315-319.

Harada M (1995) Minamata disease: methylmercury poisoning in Japan caused by environmental pollution. CRC Critical Reviews in Toxicology 25:1-24.

Hassan S, Moussa E, Abbott L (2012) The effect of methylmercury exposure on early central nervous system development in the zebrafish (*Danio rerio*) embryo. Journal of Applied Toxicology 32:707-713.

Hastings FL, Lucier GW, Klein R (1975) Methylmercury-cholinesterase interactions in rats. Environmental Health Perspectives 12:127-130.

Heideman W, Antkiewicz DS, Carney SA, Peterson RE (2005) Zebrafish and cardiac toxicology. Cardiovascular Toxicology 5:203-214.

Hu N, Sedmera D, Yost HJ, Clark EB (2000) Structure and function of the developing zebrafish heart. The Anatomical Record 260:148-157.

Kaschak E, Knopf B, Petersen JH, Bings NH, König H (2014) Biotic methylation of mercury by intestinal and sulfate-reducing bacteria and their potential role in

mercury accumulation in the tissue of the soil-living *Eisenia foetida*. Soil Biology and Biochemistry 69:202-211.

Keßler M, Just S, Rottbauer W (2012) Ion flux dependent and independent functions of ion channels in the vertebrate heart: lessons learned from zebrafish. Stem Cells International 2012:1-9.

Kimmel CB, Ballard WW, Kimmel SR, Ullmann B, Schilling TF (1995) Stages of embryonic development of the zebrafish. Developmental Dynamics 203:253-310.

Klášterská I, Ramel C (1978) The effect of methyl mercury hydroxide on meiotic chromosomes of the grasshopper *Stethophyma grossum*. Hereditas 88:255-262.

Korbas M, MacDonald TC, Pickering IJ, George GN, Krone PH (2011) Chemical form matters: differential accumulation of mercury following inorganic and organic mercury exposures in zebrafish larvae. ACS Chemical Biology 7:411-420.

Li P, Feng X, Qiu G (2010) Methylmercury exposure and health effects from rice and fish consumption: a review. International Journal of Environmental Research and Public Health 7:2666-2691.

Melançon E, Liu DW, Westerfield M, Eisen JS (1997) Pathfinding by identified zebrafish motoneurons in the absence of muscle pioneers. The Journal of Neuroscience 17:7796-7804.

Mergler D, Anderson HA, Chan LHM, Mahaffey KR, Murray M, Sakamoto M, Stern AH (2007) Methylmercury exposure and health effects in humans: a worldwide concern. AMBIO: A Journal of the Human Environment 36:3-11.

Myers GJ, Davidson PW, Cox C, Shamlaye CF, Palumbo D, Cernichiari E, Sloane-Reeves J, Wilding GE, Kost J, Huang L-S (2003) Prenatal methylmercury exposure from ocean fish consumption in the Seychelles child development study. The Lancet 361:1686-1692.

Nguyen PV, Aniksztejn L, Catarsi S, Drapeau P (1999) Maturation of neuromuscular transmission during early development in zebrafish. Journal of Neurophysiology 81:2852-2861.

Oken E, Radesky JS, Wright RO, Bellinger DC, Amarasiriwardena CJ, Kleinman KP, Hu H, Gillman MW (2008) Maternal fish intake during pregnancy, blood mercury levels, and child cognition at age 3 years in a US cohort. American Journal of Epidemiology 167:1171-1181.

Patel E, Reynolds M (2013) Methylmercury impairs motor function in early development and induces oxidative stress in cerebellar granule cells. Toxicology Letters 222:265-272.

Philbert MA, Billingsley ML, Reuhl KR (2000) Mechanisms of injury in the central nervous system. Toxicologic Pathology 28:43-53.

Samson JC, Shenker J (2000) The teratogenic effects of methylmercury on early development of the zebrafish, *Danio rerio*. Aquatic Toxicology 48:343-354.

Schmidt R, Strähle U, Scholpp S (2013) Neurogenesis in zebrafish-from embryo to adult. Neural Development 8:1749-8104.

Shih J, Fraser SE (1996) Characterizing the zebrafish organizer: microsurgical analysis at the early-shield stage. Development 122:1313-1322.

Stainier D, Lee RK, Fishman MC (1993) Cardiovascular development in the zebrafish. I. Myocardial fate map and heart tube formation. Development 119:31-40.

Stehr CM, Linbo TL, Incardona JP, Scholz NL (2006) The developmental neurotoxicity of fipronil: notochord degeneration and locomotor defects in zebrafish embryos and larvae. Toxicological Sciences 92:270-278.

Stickney HL, Barresi MJ, Devoto SH (2000) Somite development in zebrafish. Developmental Dynamics 219:287-303.

Sugamura K, Keaney Jr JF (2011) Reactive oxygen species in cardiovascular disease. Free Radical Biology and Medicine 51:978-992.

Sylvain NJ, Brewster DL, Ali DW (2011) Embryonic ethanol exposure alters synaptic properties at zebrafish neuromuscular junctions. Neurotoxicology and Teratology 33:313-321.

Tardif J-C (2009) Heart rate and atherosclerosis. European Heart Journal Supplements 11:D8-D12.

Trasande L, Landrigan PJ, Schechter C (2005) Public health and economic consequences of methyl mercury toxicity to the developing brain. Environmental Health Perspectives 113:590-596.

Vahter M, Mottet NK, Friberg L, Lind B, Shen DD, Burbacher T (1994) Speciation of mercury in the primate blood and brain following long-term exposure to methyl mercury. Toxicology and Applied Pharmacology 124:221-229.

Valencia A, Morán J (2004) Reactive oxygen species induce different cell death mechanisms in cultured neurons. Free Radical Biology and Medicine 36:1112-1125.

Waterman RE (1969) Development of the lateral musculature in the teleost, *Brachydanio rerio*: a fine structural study. American Journal of Anatomy 125:457-493.

Westerfield M (2000) The zebrafish book: a guide for the laboratory use of zebrafish (*Brachydanio rerio*). Eugene, OR: University of Oregon press.

Yang L, Ho NY, Müller F, Strähle U (2010) Methyl mercury suppresses the formation of the tail primordium in developing zebrafish embryos. Toxicological Sciences 115:379-390.

Zahir F, Rizvi SJ, Haq SK, Khan RH (2006) Effect of methyl mercury induced free radical stress on nucleic acids and protein: Implications on cognitive and motor functions. Indian Journal of Clinical Biochemistry 21:149-152.